



Original article

Chiral 3-(4,5-dihydrooxazol-2-yl)phenyl alkylcarbamates as novel FAAH inhibitors: Insight into FAAH enantioselectivity by molecular docking and interaction fields

Mikko J. Myllymäki^a, Heikki Käsnänen^{b,c}, Antti O. Kataja^a, Maija Lahtela-Kakkonen^b, Susanna M. Saario^b, Antti Poso^b, Ari M.P. Koskinen^{a,*}^a Department of Chemistry, Helsinki University of Technology, P.O. Box 6100, FI-02015 Espoo, TKK, Finland^b Department of Pharmaceutical Chemistry, University of Kuopio, P.O. Box 1627, FI-70211 Kuopio, Finland^c Division of Pharmaceutical Chemistry, University of Helsinki, P.O. Box 56, FI-000014 Helsinki, Finland

ARTICLE INFO

Article history:

Received 24 March 2009

Received in revised form

4 May 2009

Accepted 14 May 2009

Available online 22 May 2009

Keywords:

FAAH inhibitor

Fatty acid amide hydrolase

Carbamate

Enantiomeric pair

ABSTRACT

Fatty acid amide hydrolase (FAAH) and monoglyceride lipase (MGL) are the main enzymes responsible for the hydrolysis of endogenous cannabinoids *N*-arachidonylethanolamide (AEA) and 2-arachidonoylglycerol (2-AG), respectively. Phenyl alkylcarbamates are FAAH inhibitors with anxiolytic and analgesic activities in vivo. Herein we present for the first time the synthesis and biological evaluation of a series of chiral 3-(2-oxazoline)-phenyl *N*-alkylcarbamates as FAAH inhibitors. Furthermore, the structural background of chirality on the FAAH inhibition is explored by analyzing the protein–ligand interactions. Remarkably, 10-fold difference in potency was observed for (*R*)- and (*S*)-derivatives of 3-(5-methyl-4,5-dihydrooxazol-2-yl)phenyl cyclohexylcarbamate (**6a** vs. **6b**). Molecular modelling indicated an important interaction between the oxazoline nitrogen and FAAH active site.

© 2009 Elsevier Masson SAS. All rights reserved.

1. Introduction

The endocannabinoid system contains two major endogenous agonists, *N*-arachidonylethanolamide (AEA) [1] and 2-arachidonoylglycerol (2-AG) [2,3]. These compounds, also called endocannabinoids, activate cannabinoid receptors CB1 and CB2. Activation of these receptors has been reported to induce several biological effects [4,5] such as relief of pain [6] and anxiety [7], increase of appetite [8] and reduction of intraocular pressure [9]. Additionally, the activation of CB2 receptors is involved in the dampening of inflammation, lowering of blood pressure, and suppression of peripheral pain [10]. The cannabinoid signaling system is activated by increasing the levels of endocannabinoids upon demand, beginning from biosynthesis of endocannabinoids in postsynaptic neurons, and terminating in degradation of them [11,12]. The key enzymes responsible for the hydrolysis of endocannabinoids are fatty acid amide hydrolase (FAAH) and monoglyceride lipase (MGL, EC 3.1.1.23) [13,14]. FAAH is mainly

responsible for hydrolysis of AEA to arachidonic acid and ethanolamine, and MGL for hydrolysis of 2-AG to arachidonic acid and glycerol [15–17]. Numerous potent inhibitors against FAAH have been reported, including compounds that have shown promising in vivo activity, selectivity and therapeutic effects [18–21]. Boger et al. introduced a large number of potential inhibitors based on α -ketoheterocycles (e.g. OL-135, Fig. 1) that reversibly form hemiketals with the active site serine [22]. *N*-Alkylcarbamates constitute a second widely explored class of inhibitors, including the well studied compound URB597 (Fig. 1) by Piomelli et al. [7,23,24]. Inhibition by *N*-alkylcarbamates is based on irreversible acylation of the active site serine [25]. Recently reported other structure families with inhibitory activity against FAAH include (thio)hydantoin [26], piperidine- and piperazine ureas [27,28], sulfonyl derivatives [29] and boronic acid derivatives [30].

To our knowledge, thus far no systematic study on the effect of chirality on the activity of FAAH inhibitors has been presented. The stereoselectivity of FAAH has been explored briefly: while studying AEA derivatives as FAAH substrates, Makriyannis et al. found that within the enantiomeric pairs of certain methanandamides the ones having higher affinity towards CB1 receptor were also less

* Corresponding author. Tel.: +358 9 451 2526; fax: +358 9 451 2538.

E-mail address: ari.koskinen@tkk.fi (A.M.P. Koskinen).

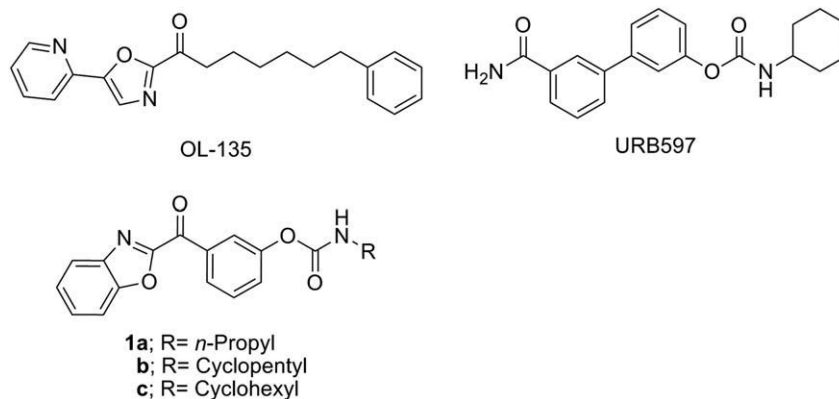


Fig. 1. FAAH inhibitors OL-135 and URB597 and lead compounds of this study (1a–c).

susceptible for FAAH hydrolysis [31]. This information, together with the stereoselectivity of the proteins in general, led us to design and study a series of carbamate enantiomeric pairs as potential FAAH inhibitors.

In the present study, novel *N*-alkylcarbamates were synthesized based upon compounds **1a–c** (Fig. 1) reported in our previous study [32]. Compounds **1a–c** inhibit FAAH with IC₅₀ values of 109, 28 and 47 nM, respectively.

The optimization of the heterocyclic portion of compounds **1a–c** was carried out by preparing compounds **2a–3c** (Table 1). 2-(4,5-Dihydro)-oxazolyl moiety has been widely utilized in ligands of the stereoselective catalysts proving their high chemical stability in various chemical environments [33]. Thus the potential importance of stereochemistry in FAAH inhibition was investigated by preparing chiral 2-oxazoline derivatives of **3c** (compounds **4b–7**). The enantiopurity of chiral compounds was determined using chiral normal phase HPLC. Compounds **2a–7** (Table 1) were consequently tested for their ability to inhibit both FAAH and MGL. Inhibition of FAAH activity was assayed in rat cerebrium homogenate using [³H]-radiolabelled AEA as a substrate. Enzyme inhibition studies for MGL were conducted in rat cerebellar membranes using 2-AG as a substrate. The formation of arachidonic acid, the hydrolysis product of 2-AG, was measured by reversed-phase HPLC. Compounds **2c**, **6a** and **6b** were tested for inhibition of human recombinant MGL (Cayman Chemical) catalyzed hydrolysis of [³H]-labelled 2-oleoylglycerol. The results of the in vitro experiments are summarized in Table 1. In addition, to understand the structural background of chirality on the FAAH inhibition, the enantiomeric pairs were docked to the FAAH active site, and the protein–ligand interactions were further analyzed with the aid of molecular interaction fields (MIFs).

2. Chemistry

The synthesis of compounds **2a–c** is presented in Scheme 1. Aminophenol **8a**, 2-amino-3-hydroxypyridine **8b** and 2-amino-3-hydroxypyrimidine **14** were condensed with 3-hydroxybenzoic acid [34]. Compound **14** was prepared in four steps from methyl methoxyacetate **10** [35,36]. Phenols **9a–b** and **15** were carbamoylated by refluxing them with isocyanates and triethylamine in toluene.

Scheme 2 illustrates the synthesis of compounds **3a–7**. 3-(2-Oxazoline)-phenol **16** was prepared via the method described by Vorbrüggen et al. [37]. Compound **17** was prepared by condensing 3-cyanophenol with 2-amino-2-methylpropanol using bismuth triflate catalysis under microwave irradiation [38]. Unfortunately this method gave poor yields. Thus for the preparation of intermediates

18a–e, the method by Witte and Seeliger [39], was applied. Compounds **19a–d** were prepared in high yields via acidic Pinner imidates [40]. Carbamates were then prepared as **2a–c**.

3. Results and discussion

We first studied the importance of ketone group between benzoxazole and 3-carbamoyl-phenyl in compound **1a**. The results of the in vitro inhibition studies showed that the absence of a ketone group within these fused bicyclic aromatic compound (e.g. **1a** vs. **2a**) decreases the FAAH-inhibition activity. Introducing a nitrogen atom into the fused oxazole-containing bicycle (**2b**) increased the inhibitory activity compared to compound **2a**. Addition of a second nitrogen did not enhance the activity: oxazolo [4,5-*d*]pyrimidin-2-yl-containing **2c** was clearly less active than **2b**. Additionally compound **3a**, which only contained the unsubstituted 2-oxazoline ring, showed good inhibitory activity against FAAH with an IC₅₀ value of 33 nM. We found earlier [32] that the cyclopentyl derivative **1b** (IC₅₀ = 28 nM) was more active than the *n*-propyl derivative **1a** (IC₅₀ = 109 nM). Similar enhancement in activity was observed for compound **3b** in comparison to **3a**. Later it was discovered that changing the carbamate *N*-alkyl group from cyclopentyl to cyclohexyl gave a further increase in activity (**3b** vs. **3c**, **4a** vs. **4b** and **4c** vs. **5a**), and hence cyclohexyl was used as the *N*-alkyl group for the rest of the series.

Furthermore, substitution in the 4-position of the oxazoline ring was found to decrease FAAH inhibition. Compound **4a** (4-dimethyl) was 5-fold and compound **4c** ((*S*)-4-Me) 10-fold less active than **3b**. A tentative presumption was made: if **4a** containing two methyl substituents at C4 has a better activity than **4b**, which only has the (*S*)-methyl, then a compound with the (*R*)-methyl at C4 should be more active against FAAH than either of these. Indeed, a clear relationship between the activity against FAAH and stereochemistry of the 4-position of oxazoline was revealed by the data of compounds **5a–f**. With methyl (**5a** vs. **5b**) and benzyl (**5c** vs. **5d**) substituents, the difference in activity between enantiomers was only 3-fold, but with methyl carboxylate (**5e** vs. **5f**) already 10-fold. This could be explained by the methyl ester's additional hydrogen bonding site or by the optimal size of the substituent. The lower activity of benzyl substituent analogs in general indicates that the enantiomeric differences in potency arise from steric hindrance. It might be that interactions between FAAH and benzyl lead to a suboptimal positioning of the carbamate functionality in the vicinity of the catalytic serine. In addition, the effect of a substituent in 5-position of oxazoline was studied with 5-methyl analogs **6a** and **b**. Compound **6b** was found to inhibit FAAH with equal potency with the most potent compound (**5f**) in the series of 4-substituted

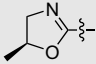
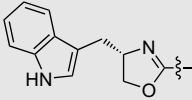
Table 1

Structures and in vitro activity of the synthesized compounds.

Compound	R ¹	R ²	FAAH IC ₅₀ , ^a μM	MGL, % of inhibition ^b
2a		<i>n</i> -Propyl	3.0 (2.6–3.6)	26
2b		<i>n</i> -Propyl	0.68 (0.59–0.78)	29
2c		<i>n</i> -Propyl	4.5 (4.0–5.2)	18 ^c
3a		<i>n</i> -Propyl	0.033 (0.028–0.038)	32
3b		Cyclopentyl	0.013 (0.011–0.014)	10 ^d
3c		Cyclohexyl	0.0012 (0.00098–0.0014)	22
4a		Cyclopentyl	0.065 (0.053–0.081)	28
4b		Cyclohexyl	0.046 (0.037–0.057)	20
4c		Cyclopentyl	0.11 (0.097–0.13)	28
5a		Cyclohexyl	0.051 (0.045–0.058)	28
5b		Cyclohexyl	0.016 (0.014–0.018)	16
5c		Cyclohexyl	2.1 (1.7–2.7)	17
5d		Cyclohexyl	0.59 (0.51–0.69)	14
5e		Cyclohexyl	0.090 (0.077–0.11)	35
5f		Cyclohexyl	0.0094 (0.0078–0.011)	25
6a		Cyclohexyl	0.073 (0.058–0.093)	13 ^c

(continued on next page)

Table 1 (continued)

Compound	R ¹	R ²	FAAH IC ₅₀ , ^a μ M	MGL, % of inhibition ^b
6b		Cyclohexyl	0.0068 (0.0056–0.0083)	14 ^c
7		Cyclohexyl	1.9 (1.6–2.4)	25

^a Values represent the mean of three independent experiments ($n = 3$) performed in duplicate (95% confidence intervals are given in parentheses).

^b Inhibition of enzymatic activity (% of control) at 100 μ M ($n = 2$).

^c Inhibition of human recombinant MGL.

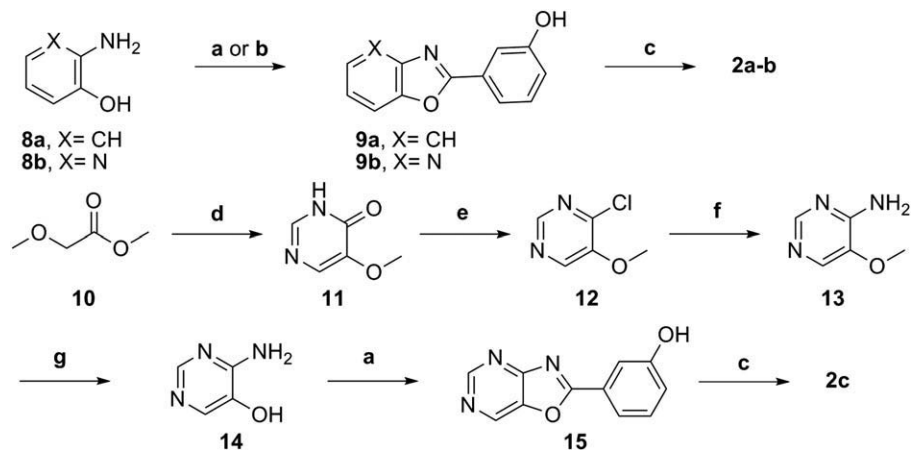
^d Inhibition of enzymatic activity (% of control) at 1 μ M ($n = 2$).

oxazolines. Furthermore, when a bulky *S*-indolyl group (**7**) was introduced at 4-position of oxazoline a significant decrease in the FAAH-inhibition activity was observed. None of the tested compounds showed significant activity against MGL at 100 μ M compound concentration, and therefore IC₅₀ values were not determined. As we found in our earlier work, in phenyl carbamates inhibiting MGL, *para*-substitution is more favorable than *meta*-substitution [32].

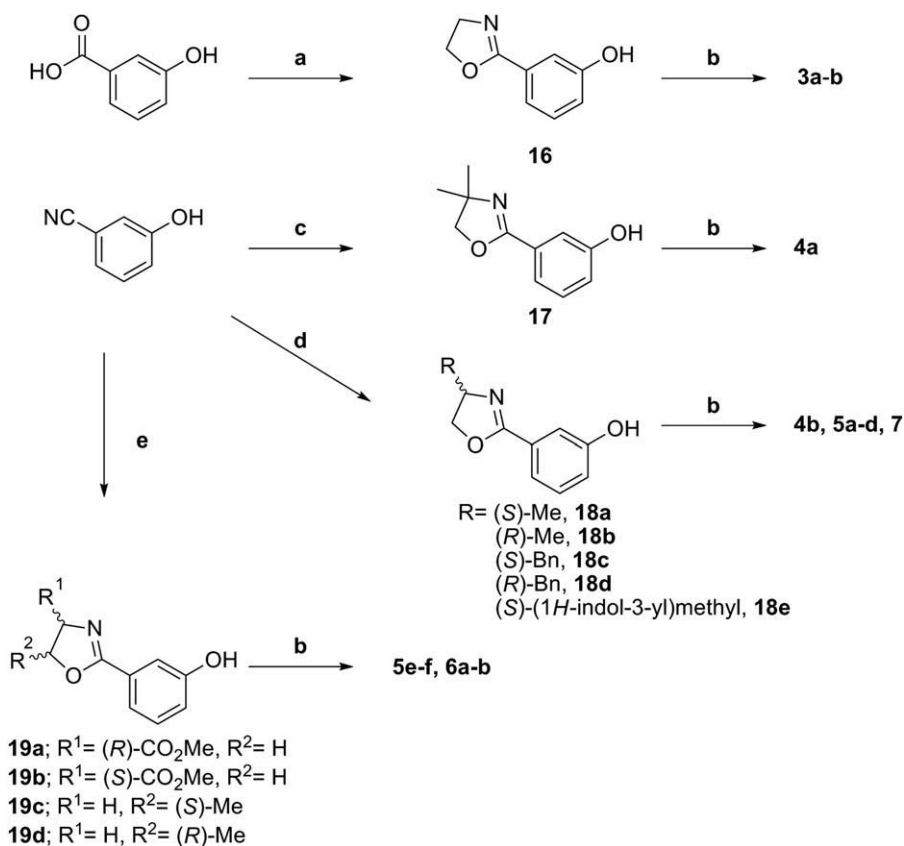
The stereochemistry of the compounds is illustrated in Fig. 2. In these Newman projections, the more active compounds **5f** and **6b** are the ones with their chiral carbon substituent “up” from the plane of the ring. This trend was also present in the enantiomeric pairs **5a** vs. **5b** and **5c** vs. **5d**. These examples suggest that the stereochemistry in the oxazoline is more important than the regiochemistry of substitution (C4 or C5). This implies that the oxazoline ring conformation is locked within the enzyme's active site. This would explain the activity difference between the enantiomeric pairs since the substituent of the chiral carbon is pointing to a specific direction and thus filling the possible hydrophobic pocket or conversely causing steric hindrance.

Molecular modelling was performed to investigate the differences in the inhibitory activities of the enantiomeric pairs. In particular, in this approach, we focused on exploring the differences arising from the protein–ligand interactions of the recognition process, as it can be assumed that the reactivity of the compounds is in similar level within the enantiomeric pairs. It should be noted

that a crystal structure of partially humanized rat FAAH with a drug-like inhibitor PF-750 [41] (PDB code 2VYA) has been published recently. This structure shows structural rearrangements in the substrate access channel region with Phe432 flipping into the acyl chain binding (ACB) channel. However, owing to our FAAH in vitro assay in rat brain homogenate, we docked the compounds to the crystal structure of murine FAAH (PDB code 1MT5) [42] with GOLD [43], and the top-ranking pose of the most abundant cluster was visualized for each enantiomer (see Experimental section for details). There is a speculation of a general FAAH binding mode of *N*-alkylcarbamates before the acylation (carbamoylation) reaction occurs [24,44,45]. In our docking study, the binding of all the enantiomers was indeed in agreement with this mode, and the ligands were positioned in a conformation where the *N*-cyclohexyl moiety is pointing towards the branching point of the ACB and substrate access channels, and forming van der Waals interactions with Phe194, Phe244, and Ile491. The oxygen of the carbamate carbonyl is accepting hydrogen bond(s) from the backbone N–H groups of the FAAH oxyanion hole residues (Ile238–Ser241) [42], thus giving rise to a conformation where the electropositive α -carbon of the ligand is residing next to the nucleophilic hydroxyl of catalytic Ser241. Moreover, the *O*-aryl part is pointing towards the cytoplasmic access (CA) cavity leading to the intracellular surface of FAAH. Noticeably, a common feature between all the enantiomeric pairs was that in enantiomers with “up”-substitutions, the oxazoline oxygen atom is pointing roughly towards the side chain of



Scheme 1. Preparation of compounds **2a–c**: a, 3-Hydroxybenzoic acid, boric acid, Na₂SO₄, *m*-xylene, autoclave, 200 °C, 16 h, 21–83%; b, 3-Hydroxybenzoic acid, MW, 250 °C, 6 min, 71–77%; c, *n*-PrNCO, Et₃N, toluene, rt or 90 °C, 20 h, 50–95%; d, i) Methyl formate, NaH, THF, 20 °C, 20 h; ii) formamidate acetate, EtOH, rt, 14 h, reflux, 24 h, 31%; e, POCl₃, reflux, 2.5 h, 86%; f, NH₃, EtOH, autoclave, 130 °C, 18 h, 75%; g, *n*-BuSH, NaH, DMF, 110 °C, 20 h, 74%.



Scheme 2. Preparation of compounds **3a–7**: a, 2-Aminoethanol, PPh₃, CCl₄, MeCN, pyridine, rt, 21 h, 29%; b, RNCO (R = *c*-pentyl or *c*-hexyl), Et₃N, toluene, rt or 90 °C, 4–24 h, 52–95%; c, 2-Amino-2-methylpropanol, BiOTf₃, MW/reflux, 3 min/4 h, 29%; d, Aminoalcohol, ZnCl₂, PhCl, reflux, 22 h, 33–90%; e, i) HCl gas, MeOH, CH₂Cl₂, 2 °C, 3 days, 92%; ii) Aminoalcohol (Et₃N in case of serine hydrochlorides), CH₂Cl₂, reflux, 2–18 h, 68–95%.

Leu192, whereas in the “down”-substituted enantiomers the oxazoline ring is flipped approximately 180°. This is most probably due to the shape of the CA cavity, and the backbone of Ser190 and the side chain of Cys269 in particular, which are sterically locking the ring in either of the aforementioned conformations. Also, it should be noted that the methyl ester of **5f** is capable of accepting a hydrogen bond from the backbone of Val270 in contrast to **5e** where no such interaction is observable (Fig. 3).

In order to further emphasize the probable interaction points in the FAAH binding site, we applied molecular interaction field (MIF) analysis by GRID [46] with probes corresponding the oxazoline ring and its substituents of the studied enantiomers. In this method, the

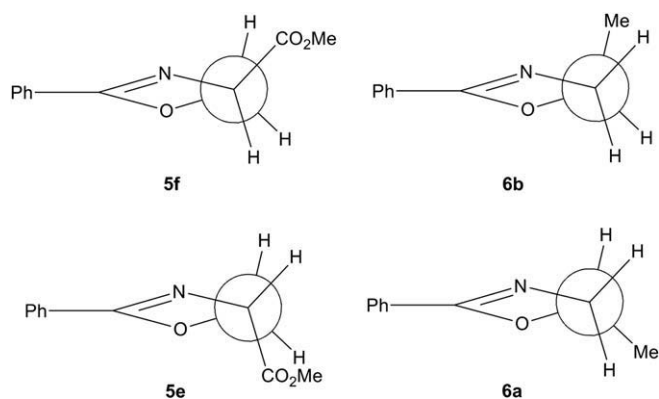


Fig. 2. Newman projections of the C4–C5 bond of oxazolines **5e–f** and **6a–b**.

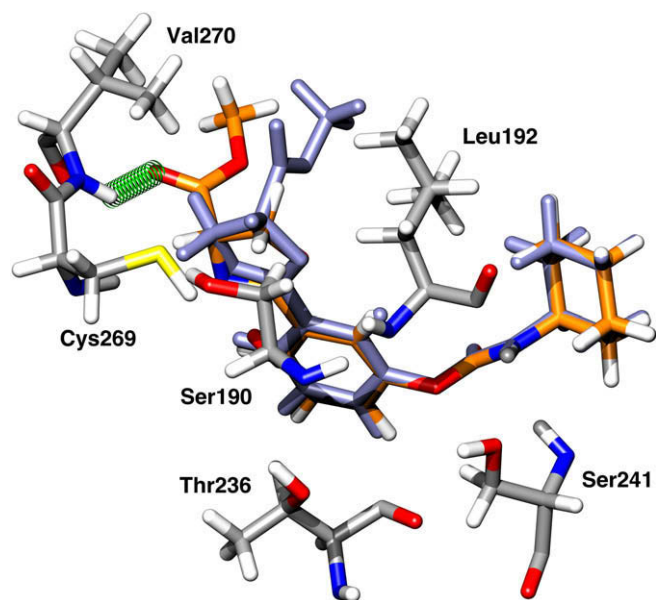


Fig. 3. The crystal structure of murine FAAH with the top-ranking docked conformations of compounds **5e** (light blue) and **5f** (carbon atoms in orange). The hydrogen bond between **5f** and Val270 is depicted in green dashed line. (For interpretation of the references to colour in this figure legend, the reader is referred to the web version of the article.)

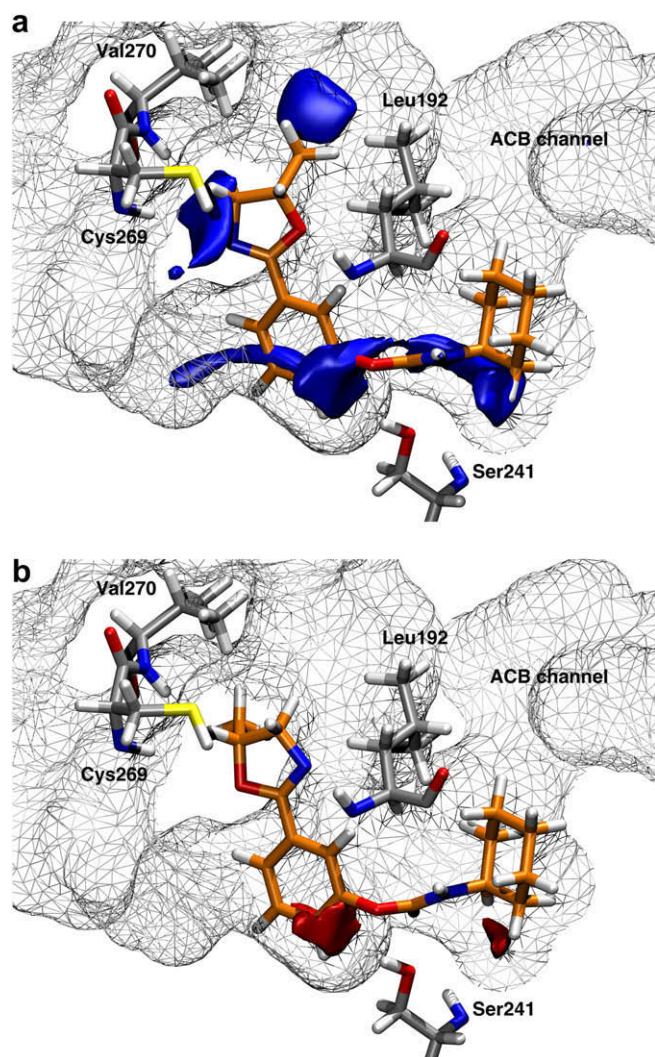


Fig. 4. The crystal structure of murine FAAH with the top-ranking docked conformations of compounds a) **6b** and b) **6a**. The GRID MIFs of sp^2 nitrogen and aromatic/aliphatic oxygen probes at contour level of -6.0 kcal/mol are colored in blue and red, respectively. The carbon atoms of the ligands are colored in orange, while those of protein in white. The wireframe presentation is illustrating the shape of the FAAH active site. In a) the distance between the oxazoline nitrogen and backbone hydrogens of Cys269 and Val270 is 2.96 Å and 3.60 Å, respectively. In b) the distance between the oxazoline oxygen and the backbone hydrogens of Cys269 and Val270 is 3.36 Å and 3.9 Å, respectively. (For interpretation of the references to colour in this figure legend, the reader is referred to the web version of the article.)

protein active site is enclosed in a grid cage, and the interaction energies between amino acid residues and probes are calculated. The resulting MIFs can be then used to determine the most favorable interaction regions in the active site. By visualizing the MIFs in the light of the docked compounds, no explanation for the inhibition activity differences arising from the oxazoline ring substituent conformations could be seen, apart from the carbonyl oxygen probe indicating a favorable interaction with Val270 backbone (corresponding to the aforementioned hydrogen bond of the methyl ester of **5f**). However, when studying the MIFs in the binding region of the oxazoline ring, the sp^2 nitrogen probe showed strong interaction with the backbone of Cys269 and Val270 (Fig. 4a). Furthermore, with the same interaction energy level, no interaction is observed with these residues and aromatic/aliphatic ether oxygen probe (Fig. 4b). This is in line with the docking results, and suggests that the “up”-substituted carbamates are forming an electrostatic interaction between the oxazoline ring nitrogen and the backbone N–H groups

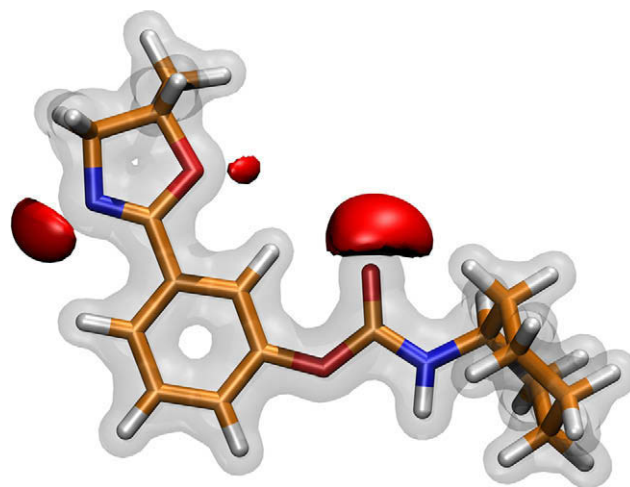


Fig. 5. The optimized structure and the electrostatic potential $V(r)$ (isopotential surface) of **6b**. The gray and red areas correspond to $+0.25$ and -0.07 eV, respectively. The minimum and maximum $V(r)$ values for **6b** are -0.1132 and $+137.3$ eV, respectively. (For interpretation of the references to colour in this figure legend, the reader is referred to the web version of the article.)

of Cys269 and Val270, whereas in “down”-substituted compounds the interaction between the ring oxygen and these residues is clearly less favorable. This type of interaction between oxazoline nitrogen and protein backbone is not uncommon, and in Relibase [47] one can find cases of similar drug–receptor interactions (e.g. [48]).

To gain confidence in this observation, we wanted to assess the electronic properties of the enantiomers in more detail by calculating the electrostatic potentials $V(r)$ s with an ab initio method. In all of the optimized structures the minima of the electrostatic potential was located in the vicinity of the oxazoline nitrogen (Fig. 5). This indirectly indicates the oxazoline nitrogen having higher interaction potential compared to the oxygen [49,50]. Thus, it seems the IC_{50} differences of the enantiomeric pairs might be indeed due to the sterical features of the FAAH active site, and the consequential electrostatic dipole–dipole interaction of the “up”-substituted oxazoline carbamates with the Cys269 and Val270 backbone N–H groups.

4. Conclusion

In conclusion, a series of chiral 3-oxazolinyphenyl *N*-alkylcarbamates were prepared and tested for their in vitro inhibitory activity against FAAH and MGL. In this series, enantiomers having their chiral center substituent “up” from plane of the oxazoline ring (**5b**, **5d**, **5f**, **6b**) were found to be more potent FAAH inhibitors than corresponding “down” enantiomers. The most potent chiral compound, (*R*)-3-(5-methyl-4,5-dihydrooxazol-2-yl)phenyl cyclohexylcarbamate (**6b**), inhibited FAAH with approximately 10-fold higher potency (IC_{50} value: 6.8 nM) than the corresponding (*S*)-enantiomer (**6a**, IC_{50} value: 73 nM). In addition, non-substituted oxazoline derivative (**3b**, IC_{50} value: nM) was found to be more potent than any of the corresponding substituted compounds. None of the compounds presented significantly inhibited MGL activity. Since the carbamate based FAAH inhibitors have been reported to have several off-targets [19,25,51] the selectivity of chiral 3-oxazolinyphenyl *N*-alkylcarbamates would be important issue to study in more detail in the future. In molecular modelling studies, the combined docking and molecular interaction field analysis emphasized the importance of heterocycle interaction with Cys269 and Val270 of FAAH, and also highlighted the steric features of the FAAH active site. These findings could provide

valuable information for further development of more selective FAAH inhibitors.

5. Experimental protocols

5.1. Chemistry

Commercially available starting materials were used without further purification. All dry reactions were performed under argon in flame-dried glassware and solvents were distilled. In microwave reactions CEM Discover -microwave reactor was used. Analytical thin-layer chromatography was carried out on Merck silica gel F254 (60 Å, 40–63 µm, 230–400 mesh) precoated aluminium sheets and detected under UV light. Purification of reaction products was carried out by flash chromatography (FC) on J. T. Bakers silica gel for chromatography (pore size 60 Å, particle size 50 nm). The ^1H NMR and ^{13}C NMR spectra were recorded on a Bruker Avance 400 spectrometer operating at 400 MHz for ^1H and 100 MHz for ^{13}C . Chemical shifts are reported in ppm on the δ scale from an internal standard (TMS 0.00 ppm) or residual solvent (CDCl_3 7.26 and 77.0 ppm; $\text{DMSO}-d_6$ 2.50 and 39.52 ppm). Melting points were determined in open capillaries using Stuart SMP3 and are uncorrected. Optical rotation data were recorded on Perkin Elmer 343 polarimeter using Na lamp (589 nm) and 100 mm cuvette at room temperature. HRMS were recorded on Waters Micromass LCT Premier (ESI) spectrometer. Chiral HPLC analysis was carried out using Waters pump and UV detector (254 nm) and Daicel Chiralcel OD analytical chiral column. Eluent used was 20% 2-propanol in hexane with flow rate 0.5 mL/min. Retention time (R_t) and ee-% are reported. Elemental analyses (CHN) were recorded using a Perkin Elmer 2400 CHN-elemental analyzer. Analyses indicated by the symbols of the elements were within $\pm 0.4\%$ of the theoretical values.

5.1.1. 3-Benzo[d]oxazol-2-yl-phenol (**9a**) [52,53]

3-Hydroxybenzoic acid (840 mg, 6.2 mmol, 100 mol-%), 2-aminophenol (**8a**, 680 mg, 6.1 mmol, 100 mol-%), boric acid (380 mg, 6.1 mmol, 100 mol-%) and Na_2SO_4 (8 g, 56 mmol, 900 mol-%) were stirred in *m*-xylene (60 mL) in an autoclave at 200 °C for 16 h. The cooled mixture was poured into sat. aq. NaHCO_3 (100 mL) and extracted with EtOAc (3×100 mL). Combined organic phases were washed with water (100 mL) and brine (100 mL), dried with Na_2SO_4 , filtered and evaporated. The resulting red solid (1.36 g) was purified by FC (20% EtOAc in hex) and recrystallized (EtOAc/hex) giving **9a** (1.07 g, 83%) as a white solid: mp. 238–239 °C, R_f (50% EtOAc in hex) 0.5; ^1H NMR ($\text{DMSO}-d_6$) 9.97 (s, 1H), 7.81–7.77 (m, 1H), 7.64 (dt, 1H, $J = 7.8, 1.1$ Hz), 7.60–7.59 (m, 1H), 7.45–7.38 (m, 3H), 7.02 (ddd, 1H, $J = 8.2, 2.5, 0.8$ Hz); ^{13}C NMR ($\text{DMSO}-d_6$) 162.3, 157.9, 150.2, 141.5, 130.6, 127.5, 125.5, 124.9, 119.8, 119.2, 118.1, 113.7, 110.9.

5.1.2. Procedure for preparation of carbamates: 3-(benzo[d]oxazol-2-yl)phenyl propylcarbamate (**2a**)

Compound **9a** (79 mg, 0.37 mmol, 100 mol-%), propylisocyanate (158 mg, 1.85 mmol, 500 mol-%) and Et_3N (37 mg, 0.37 mmol, 100 mol-%) were stirred in toluene (4 mL) at rt for 16 h. The mixture was diluted with EtOAc (5 mL) and filtered through a pad of silica. The crude material was recrystallized (EtOAc/hex) giving **2a** (84 mg, 77%) as white crystals: mp. 144–145 °C, R_f (EtOAc) 0.5; ^1H NMR (CDCl_3) 8.09 (d, 1H, $J = 7.8$ Hz), 8.03 (s, 1H), 7.78–7.74 (m, 1H), 7.59–7.55 (m, 1H), 7.50 (t, 1H, $J = 8.0$ Hz), 5.17 (br s, 1H), 3.26 (q, 2H, $J = 6.7$ Hz), 1.62 (sext, 2H, $J = 7.3$ Hz), 0.98 (t, 3H, $J = 7.4$ Hz); ^{13}C NMR (CDCl_3) 162.2, 154.2, 151.5, 150.7, 142.0, 129.8, 128.3, 125.3, 124.8, 124.6, 124.3, 120.9, 120.1, 110.6, 43.0, 23.0, 11.2; Anal. $\text{C}_{17}\text{H}_{16}\text{N}_2\text{O}_3$ (C, H, N).

5.1.3. 3-(Oxazolo[4,5-b]pyridin-2-yl)phenol (**9b**) [34,54]

3-Hydroxybenzoic acid (250 mg, 1.8 mmol, 150 mol-%) and 2-amino-3-hydroxypyridine (**8b**, 130 mg, 1.2 mmol, 100 mol-%) were microwave-irradiated (300 W, 4 min ramp to 250 °C, hold 2 min). The tan solid was dissolved to MeOH/EtOAc (1:1, 10 mL), poured to sat. aq. NaHCO_3 (30 mL) and extracted with EtOAc (3×50 mL). Combined organic phases were washed with water (50 mL) and brine (50 mL), dried (Na_2SO_4), filtered and evaporated. The crude material was purified by FC (50% EtOAc in hex) and recrystallized (EtOAc/hex) giving **9b** (195 mg, 77%) as a white solid: mp. 203–204 °C, R_f (EtOAc) 0.5; ^1H NMR ($\text{DMSO}-d_6$) 10.02 (s, 1H), 8.55 (dd, 1H, $J = 4.9, 1.4$ Hz), 8.24 (dd, 1H, $J = 8.2, 1.4$ Hz), 7.69 (app dt, 1H, $J = 7.7, 1.2$ Hz), 7.64 (t, 1H, $J = 2.0$ Hz), 7.48–7.43 (m, 2H), 7.08 (ddd, 1H, $J = 8.2, 2.5, 0.9$ Hz); ^{13}C NMR ($\text{DMSO}-d_6$) 165.0, 158.1, 155.6, 146.7, 142.9, 130.8, 127.1, 121.0, 120.2, 119.3, 118.7, 114.1.

5.1.4. 3-(Oxazolo[4,5-b]pyridin-2-yl)phenyl propylcarbamate (**2b**)

White solid (93 mg, 78%): mp. 146–147 °C, R_f (EtOAc) 0.5; ^1H NMR (CDCl_3) 8.59 (dd, 1H, $J = 4.9, 1.3$ Hz), 8.17 (d, 1H, $J = 7.8$ Hz), 8.10–8.08 (m, 1H), 7.86 (dd, 1H, $J = 8.1, 1.3$ Hz), 7.54 (t, 1H, $J = 8.0$ Hz), 7.39–7.36 (m, 1H), 7.31 (dd, 1H, $J = 8.1, 4.9$ Hz), 5.19 (br s, 1H), 3.28 (q, 2H, $J = 6.7$ Hz), 1.64 (sext, 2H, $J = 7.2$ Hz), 1.00 (t, 3H, $J = 7.4$ Hz); ^{13}C NMR (CDCl_3) 164.9, 156.2, 154.0, 151.5, 146.8, 143.1, 130.0, 127.7, 125.8, 124.9, 121.2, 120.2, 118.2, 43.0, 23.0, 11.2; Anal. $\text{C}_{16}\text{H}_{15}\text{N}_3\text{O}_3$ (C, H, N).

5.1.5. 5-Methoxypyrimidin-4(3H)-one (**11**) [55]

Methyl 2-methoxyacetate (**10**, 10.4 g, 100 mmol, 100 mol-%) and methyl formate (7.2 g, 120 mmol, 120 mol-%) were added to a mixture of sodium hydride (5.6 g of 60% dispersion in oil, 140 mmol, 140 mol-%) in dry THF (150 mL) and stirred for 20 h keeping the temperature of the mixture at 20 °C by water bath. After formation of white solid, dry Et_2O (100 mL) was added and the mixture was filtered. The solid (18.6 g) was dried under reduced pressure and added to a mixture of formamidine acetate (10.4 g, 100 mmol, 100 mol-%) in EtOH (200 mL) at rt. The mixture was stirred for 14 h at rt and refluxed for 24 h. Water (70 mL) was added and the mixture was acidified with AcOH (25 mL) from pH 10 to 5. Ethanol was evaporated and the residue was extracted with CHCl_3 (10×100 mL) and EtOAc: Et_2O (2:1, 3×100 mL). Combined organic phases were dried over MgSO_4 , filtered and evaporated. Crystallization of the crude product (MeOH:hex) gave **11** (3.9 g, 31%) as off-white solid: mp. 216–217 °C; R_f (10% MeOH in CH_2Cl_2) 0.2; ^1H NMR ($\text{DMSO}-d_6$) 12.51 (br s, 1H), 7.81 (s, 1H), 7.52 (s, 1H), 3.73 (s, 3H).

5.1.6. 4-Chloro-5-methoxypyrimidine (**12**) [53]

Compound **11** (2.6 g, 20.6 mmol, 100 mol-%) was treated with phosphorus oxychloride (17 mL, 180 mmol, 900 mol-%) at 0 °C. The mixture was refluxed for 2.5 h, cooled to 30–40 °C and unreacted POCl_3 was removed under reduced pressure. Ice-cold water (50 mL) was added and pH was adjusted to 7 with K_2CO_3 (10 g). The mixture was extracted with EtOAc: Et_2O (3:1, 3×150 mL), organic phases were combined, dried (MgSO_4) and filtered through a pad of silica (eluted with EtOAc). Evaporation of the solvents resulted in compound **12** (2.6 g, 86%) as a yellow solid; mp. 63–64 °C; R_f (EtOAc) 0.5; ^1H NMR (CDCl_3) 8.60 (s, 1H), 8.30 (s, 1H), 4.00 (s, 3H).

5.1.7. 5-Methoxypyrimidin-4-amine (**13**) [56]

The mixture of **12** (3.4 g, 24 mmol, 100 mol-%) in EtOH (30 mL) was bubbled with dry NH_3 gas for 30 min at 0 °C. The mixture was poured to autoclave and stirred at 130 °C for 18 h. Cooling and evaporation resulted in tan residue which was dissolved to CHCl_3

(100 mL) and brine (100 mL) and extracted with CHCl_3 (3×100 mL). Combined organic phases were dried over MgSO_4 , filtered and evaporated giving **13** (2.2 g, 75%) as a yellow solid; mp. 117–119 °C; R_f (10% MeOH in CH_2Cl_2) 0.4; ^1H NMR ($\text{DMSO}-d_6$) 7.99 (s, 1H), 7.79 (s, 1H), 6.68 (s, 2H), 3.80 (s, 3H).

5.1.8. 4-Aminopyrimidin-5-ol (**14**) [57]

The mixture of **13** (280 mg, 2.2 mmol, 100 mol-%) in dry DMF (15 mL) was treated with NaH (215 mg, washed with hexanes from 60% mineral oil dispersion, 9.0 mmol, 400 mol-%) at rt. The mixture was cooled by ice bath and *n*-BuSH (300 mg, 3.3 mmol, 150 mol-%) was added. The mixture was stirred at 110 °C for 20 h and evaporated to dryness. AcOH (0.25 mL) and water (2.5 mL) were added and evaporation was repeated. The residue was purified by FC (10% MeOH in CH_2Cl_2) and recrystallized (MeOH) giving **14** (181 mg, 74%) as a red solid; mp. 257–260 °C; R_f (20% MeOH in CH_2Cl_2) 0.2; ^1H NMR ($\text{DMSO}-d_6$) 9.81 (br s, 1H), 7.90 (s, 1H), 7.65 (s, 1H), 6.44 (2H).

5.1.9. 3-(Oxazolo[4,5-d]pyrimidin-2-yl)phenol (**15**)

Compound **14** (222 mg, 2.0 mmol, 100 mol-%), 3-hydroxybenzoic acid (276 mg, 2.0 mmol, 100 mol-%), boric acid (124 mg, 2.0 mmol, 100 mol-%) and Na_2SO_4 (2.5 g, 18 mmol, 900 mol-%) were stirred in *m*-xylene (20 mL) in an autoclave at 200 °C for 24 h. The cooled mixture was poured into sat. aq. NaHCO_3 (50 mL) and extracted with EtOAc (3×70 mL). Combined organic phases were dried over Na_2SO_4 , filtered and evaporated. The resulting red solid was purified by FC (50% EtOAc in hex) and recrystallized (MeOH/ CH_2Cl_2) giving **15** (92 mg, 21%) as an off-white solid: mp. 257–261 °C; R_f (EtOAc) 0.5; ^1H NMR ($\text{DMSO}-d_6$) 10.14 (s, 1H), 9.33 (s, 1H), 9.14 (s, 1H), 7.76 (d, 1H, $J = 7.7$ Hz), 7.68 (app t, 1H, $J = 1.9$ Hz), 7.49 (t, 1H, $J = 7.9$ Hz), 7.15 (dd, 1H, $J = 8.1$, 2.1 Hz); ^{13}C NMR ($\text{DMSO}-d_6$) 167.6, 161.6, 158.0, 154.9, 142.2, 139.7, 130.8, 126.2, 121.1, 119.3, 114.7; HRMS (ESI): calcd. for $[\text{M} + \text{Na}]$ $\text{C}_{11}\text{H}_7\text{N}_3\text{O}_2\text{Na}$: 236.0436, found 236.0447.

5.1.10. 3-(Oxazolo[4,5-d]pyrimidin-2-yl)phenyl propylcarbamate (**2c**)

A white solid (30 mg, 50%); mp. 161–162 °C; R_f (EtOAc) 0.5; ^1H NMR (CDCl_3) 9.20 (s, 1H), 9.01 (s, 1H), 8.2 (dt, 1H, $J = 7.87$, 1.28 Hz), 8.14 (t, 1H, $J = 1.9$ Hz), 7.58 (t, 1H, $J = 8.0$ Hz), 7.45 (ddd, 1H, $J = 8.2$, 2.3, 0.9 Hz), 5.24 (app t, 1H, $J = 5.5$ Hz), 3.28 (q, 2H, $J = 6.7$ Hz), 1.64 (sext, 2H, $J = 7.2$ Hz), 1.00 (t, 3H, $J = 7.4$ Hz); ^{13}C NMR (CDCl_3) 167.6, 162.3, 155.5, 154.0, 151.7, 142.3, 138.8, 130.2, 127.1, 126.5, 125.6, 122.0, 43.0, 23.0, 11.2; HRMS (ESI): calcd. for $[\text{M} + \text{Na}]$ $\text{C}_{15}\text{H}_{14}\text{N}_4\text{O}_3\text{Na}$: 321.0964, found 321.0951.

5.1.11. 3-(4,5-Dihydrooxazol-2-yl)-phenol (**16**) [58]

3-Hydroxybenzoic acid (1.38 g, 10 mmol, 100 mol-%), 2-aminoethanol (610 mg, 10 mmol, 100 mol-%) and Et_3N (3.0 g, 30 mmol, 300 mol-%) were stirred in pyridine (20 mL) and MeCN (30 mL) at 22 °C for 40 min. CCl_4 (6.15 g, 40 mmol, 400 mol-%) was added followed by dropwise admission of PPh_3 in pyridine–MeCN (1:1, 80 mL) during 2 h keeping the temperature of the mixture between 22 and 24 °C. The mixture was stirred for 18 h, concentrated by rotavapor to ca. 40 mL, diluted with aq. ammonia (25%, 100 mL) and extracted with EtOAc (3×100 mL). Combined organic phases were washed with sat. aq. CuSO_4 (100 mL), water (100 mL) and brine (100 mL), dried (Na_2SO_4), filtered and evaporated. The crude product was purified by FC (0–4% MeOH in CH_2Cl_2) giving **16** (479 mg, 29%) as a white solid: mp. 188–189 °C; R_f (EtOAc) 0.5; ^1H NMR ($\text{DMSO}-d_6$) 9.70 (s, 1H), 7.30–7.23 (m, 3H), 6.91 (d, 1H, $J = 8.1$ Hz), 4.36 (t, 2H, $J = 9.5$ Hz), 3.92 (t, 2H, $J = 9.5$ Hz); ^{13}C NMR ($\text{DMSO}-d_6$) 163.0, 157.3, 129.7, 128.7, 118.5, 118.4, 114.3, 67.2, 54.4. This compound was later prepared in 96% yield by similar method as **19a**.

5.1.12. 3-(4,5-Dihydrooxazol-2-yl)phenyl propylcarbamate (**3a**)

White crystals (65 mg, 65%); mp. 94–95 °C; R_f (EtOAc) 0.5; ^1H NMR (CDCl_3) 7.78 (d, 1H, $J = 7.8$ Hz), 7.70 (s, 1H), 7.39 (t, 1H, $J = 8.0$ Hz), 7.29–7.24 (m, 1H), 5.05 (br s, 1H), 4.43 (app t, 2H, $J = 9.5$ Hz), 4.06 (app t, 2H, $J = 9.5$ Hz), 3.24 (q, 2H, $J = 6.7$ Hz), 1.60 (sext, 2H, $J = 7.3$ Hz), 0.97 (t, 3H, $J = 7.4$ Hz); ^{13}C NMR (CDCl_3) 163.9, 150.9, 129.1, 128.9, 124.9, 124.6, 121.4, 67.6, 54.8, 42.9, 23.0, 11.1; Anal. $\text{C}_{13}\text{H}_{16}\text{N}_2\text{O}_3$ (C, H, N).

5.1.13. 3-(4,5-Dihydrooxazol-2-yl)phenyl cyclopentylcarbamate (**3b**)

White crystals (48 mg, 70%); mp. 166–168 °C; R_f (10% Et₂O in CH_2Cl_2) 0.4; ^1H NMR ($\text{DMSO}-d_6$) 7.86 (d, 1H, $J = 7.1$ Hz), 7.69 (d, 1H, $J = 7.7$ Hz), 7.53 (s, 1H), 7.47 (t, 1H, $J = 7.9$ Hz), 7.28 (dd, 1H, $J = 1.5$, 8.1 Hz), 4.41 (t, 2H, $J = 9.5$ Hz), 3.96 (t, 2H, $J = 9.5$ Hz), 3.88–3.79 (m, 1H), 1.89–1.79 (m, 2H), 1.72–1.61 (m, 2H), 1.57–1.44 (m, 4H); ^{13}C NMR ($\text{DMSO}-d_6$) 162.3, 153.4, 151.0, 129.7, 128.6, 124.7, 124.1, 120.9, 67.5, 54.4, 52.4, 32.2, 23.3; Anal. $\text{C}_{15}\text{H}_{18}\text{N}_2\text{O}_3$ (C, H, N).

5.1.14. 3-(4,5-Dihydrooxazol-2-yl)phenyl cyclohexylcarbamate (**3c**)

White cotton-like crystals (100 mg, 71%); mp. 151–152 °C; R_f (5% MeOH in CH_2Cl_2) 0.54; ^1H NMR (CDCl_3) 7.78 (d, 1H, $J = 8.0$ Hz), 7.71–7.69 (s, 1H), 7.39 (t, 1H, $J = 7.9$ Hz), 7.28–7.23 (m, 1H), 4.94 (d, 1H, $J = 7.0$ Hz), 4.42 (t, 2H, $J = 9.5$ Hz), 4.05 (t, 2H, $J = 9.5$ Hz), 3.63–3.50 (m, 1H), 2.07–1.96 (m, 2H), 1.79–1.70 (m, 2H), 1.67–1.58 (m, 1H), 1.44–1.31 (m, 2H), 1.28–1.14 (m, 3H); ^{13}C NMR (CDCl_3) 163.9, 153.3, 151.0, 129.2, 129.0, 124.9, 124.6, 121.5, 67.7, 54.9, 50.2, 33.2, 25.4, 24.7; Anal. $\text{C}_{16}\text{H}_{20}\text{N}_2\text{O}_3$ (C, H, N).

5.1.15. 3-(4,4-Dimethyl-4,5-dihydrooxazol-2-yl)phenol (**17**) [37]

This compound was synthesized in two different methods: Method 1: 3-cyanophenol (237 mg, 2.0 mmol, 100 mol-%), 2-amino-2-methylpropanol (450 μL , 4.0 mmol, 200 mol-%) and bismuth trifluoromethylsulfonate (64.5 mg, 0.1 mmol, 5 mol-%) were microwave-irradiated in a closed vessel (2×60 s at 50 W, 1×60 s at 60 W). The resulting mixture was diluted with EtOAc and purified by FC (40% EtOAc in hex).

Method 2: 3-cyanophenol (237 mg, 2.0 mmol, 100 mol-%), 2-amino-2-methylpropanol (450 μL , 4.0 mmol, 200 mol-%) and bismuth trifluoromethylsulfonate (64.5 mg, 0.1 mmol, 5 mol-%) were refluxed for 3 h. Crops from both reactions were combined and recrystallized from toluene giving **17** (190 mg, 25% overall yield) as a white solid: mp. 159–161 °C; R_f (65% EtOAc in hex) 0.28; ^1H NMR ($\text{DMSO}-d_6$) 9.66 (s, 1H), 7.28–7.21 (m, 3H), 6.92–6.88 (m, 1H), 4.07 (m, 2H), 1.26 (m, 6H). This compound was later prepared in 90% yield by similar method as **18a**.

5.1.16. 3-(4,4-Dimethyl-4,5-dihydrooxazol-2-yl)phenyl cyclopentylcarbamate (**4a**)

White needles (73 mg, 48%); mp. 139–141 °C; R_f (10% Et₂O in CH_2Cl_2) 0.27; ^1H NMR ($\text{DMSO}-d_6$) 7.76 (d, 1H, $J = 7.7$ Hz), 7.70 (s, 1H), 7.38 (dd, 1H, $J = 7.9$ Hz), 7.23 (d, 2H, $J = 8.1$ Hz), 4.98 (d, 1H, $J = 6.4$ Hz), 4.10 (s, 2H), 4.07–4.00 (m, 1H), 2.06–1.98 (m, 2H), 1.76–1.69 (m, 2H), 1.66–1.60 (m, 2H), 1.53–1.44 (m, 2H), 1.37 (s, 6H); ^{13}C NMR ($\text{DMSO}-d_6$) 161.3, 153.7, 150.9, 129.4, 129.1, 125.0, 124.5, 121.6, 79.1, 67.6, 53.0, 33.1, 28.4, 23.5; Anal. $\text{C}_{17}\text{H}_{22}\text{N}_2\text{O}_3$ (C, H, N).

5.1.17. 3-(4,4-Dimethyl-4,5-dihydrooxazol-2-yl)phenyl cyclohexylcarbamate (**4b**)

White crystals (176 mg, 56%); mp. 154–155 °C; R_f (5% MeOH in CH_2Cl_2) 0.67; ^1H NMR (CDCl_3) 7.76 (d, 1H, $J = 7.8$ Hz), 7.72–7.69 (m, 1H), 7.37 (t, 1H, $J = 7.9$ Hz), 7.23 (dd, 1H, $J = 8.1$, 1.4 Hz), 4.96 (d, 1H, $J = 7.5$ Hz), 4.09 (s, 2H), 3.62–3.49 (m, 1H), 2.06–1.95 (m, 2H), 1.79–1.69 (m, 2H), 1.66–1.58 (m, 2H), 1.44–1.31 (m, 7H), 1.28–1.13 (m, 3H); ^{13}C NMR (CDCl_3) 161.3, 153.4, 151.0, 129.3, 129.1, 124.9, 124.5, 121.6, 79.2, 67.6, 50.1, 33.2, 28.4, 25.4, 24.7; Anal. $\text{C}_{18}\text{H}_{24}\text{N}_2\text{O}_3$ (C, H, N).

5.1.18. Procedure for preparation of **18a-e**

5.1.18.1. (S)-3-(4-Methyl-4,5-dihydrooxazol-2-yl)phenol (18a). Zinc chloride (48 mg, 0.35 mmol, 10 mol-%) was melted in a 50 mL flask under high vacuum. 3-Cyanophenol (413 mg, 3.46 mmol, 100 mol-%) and chlorobenzene (10 mL) were added and heated up to reflux under argon atmosphere. (S)-2-Aminopropanol (510 μ L, 6.5 mmol, 190 mol-%) was added and the mixture was refluxed for 22 h. The mixture was cooled to rt and filtered through a pad of silica with EtOAc and purified by FC (33% EtOAc in hex) and recrystallized from EtOAc:hex giving **18a** (317 mg, 52%) as white needles: mp. 125–126 °C; R_f (50% EtOAc in hex) 0.31; $[\alpha]_D$ 48 (c = 0.5, CDCl_3); ^1H NMR (CDCl_3) 9.45 (br s, 1H), 7.45 (dd, 1H, J = 2.3, 1.6 Hz), 7.30 (td, 1H, J = 7.7, 1.3 Hz), 7.18 (t, 1H, J = 7.9 Hz), 6.95 (ddd, 1H, J = 8.1, 2.5, 1.0 Hz), 4.53 (dd, 1H, J = 9.4, 8.0 Hz), 4.45–4.36 (m, 1H), 3.96 (t, 1H, J = 7.9 Hz), 1.33 (d, 3H, J = 6.6 Hz); ^{13}C NMR (CDCl_3) 164.6, 156.9, 129.6, 128.0, 119.8, 119.5, 115.1, 74.2, 61.2, 21.1; Anal. $\text{C}_{10}\text{H}_{11}\text{NO}_2$ (C, H, N).

5.1.19. (S)-3-(4-Methyl-4,5-dihydrooxazol-2-yl)phenyl cyclopentyl-carbamate (**4c**)

White crystals (83 mg, 51%): mp. 139–142 °C; R_f (15% Et_2O in CH_2Cl_2) 0.33; $[\alpha]_D$ –54 (c = 0.5, CHCl_3); ^1H NMR (CDCl_3) 7.77 (d, 1H, J = 7.7 Hz), 7.70 (s, 1H), 7.38 (t, 1H, J = 8.0 Hz), 7.24 (d, 1H, J = 8.1 Hz), 5.04 (d, 1H, J = 6.6 Hz), 4.51 (dd, 1H, J = 9.3, 8.1 Hz), 4.41–4.32 (m, 1H), 4.09–4.00 (m, 1H), 3.94 (t, 1H, J = 7.9 Hz), 2.06–1.97 (m, 2H), 1.75–1.56 (m, 4H), 1.53–1.44 (m, 2H), 1.35 (d, 3H, J = 6.6 Hz); ^{13}C NMR (CDCl_3) 162.7, 160.1, 153.7, 151.0, 129.1, 125.0, 124.6, 121.6, 74.1, 62.0, 53.0 (rotam. 52.1), 33.1 (rotam. 33.6), 23.5, 21.4; Anal. $\text{C}_{16}\text{H}_{20}\text{N}_2\text{O}_3$ (C, H, N).

5.1.20. (S)-3-(4-Methyl-4,5-dihydrooxazol-2-yl)phenyl cyclohexyl-carbamate (**5a**)

White crystals (94 mg, 65%): mp. 133–135 °C; R_f (50% EtOAc in hex) 0.40; $[\alpha]_D$ –49 (c = 0.5, CHCl_3); ^1H NMR (CDCl_3) 7.77 (d, 1H, J = 7.7 Hz), 7.70 (s, 1H), 7.38 (t, 1H, J = 7.9 Hz), 7.26–7.23 (m, 1H), 4.92 (d, 1H, J = 7.3 Hz), 4.51 (dd, 1H, J = 9.2, 8.2 Hz), 4.42–4.32 (m, 1H), 3.94 (t, 1H, J = 7.9 Hz), 3.61–3.51 (m, 1H), 2.05–1.97 (m, 2H), 1.78–1.70 (m, 2H), 1.66–1.59 (m, 1H), 1.43–1.32 (m, 2H), 1.35 (d, 3H, J = 6.6 Hz), 1.28–1.15 (m, 3H); ^{13}C NMR (CDCl_3) 162.8, 153.4, 151.0, 129.1 (2C), 125.0, 124.6, 121.6, 74.1, 62.0, 50.1, 33.2, 25.4, 24.7, 21.4; Rt 60 min, 93 ee-%; Anal. $\text{C}_{17}\text{H}_{22}\text{N}_2\text{O}_3$ (C, H, N).

5.1.21. (R)-3-(4-Methyl-4,5-dihydrooxazol-2-yl)phenol (**18b**)

White needles (283 mg, 57%): mp. 126–127 °C; R_f (50% EtOAc in hex) 0.19; $[\alpha]_D$ –46 (c = 0.5, CHCl_3); ^1H NMR (CDCl_3) 9.46 (br s, 1H), 7.44 (dd, 1H, J = 2.4, 1.6 Hz), 7.29 (td, 1H, J = 7.7, 1.3 Hz), 7.18 (t, 1H, J = 7.9 Hz), 6.95 (ddd, 1H, J = 8.1, 2.6, 1.0 Hz), 4.53 (dd, 1H, J = 9.5, 8.1 Hz), 4.45–4.36 (m, 1H), 3.96 (t, 1H, J = 7.9 Hz), 1.33 (d, 3H, J = 6.6 Hz); ^{13}C NMR (CDCl_3) 164.5, 156.9, 129.6, 127.9, 119.8, 119.5, 115.0, 74.2, 61.1, 21.1; Anal. $\text{C}_{10}\text{H}_{11}\text{NO}_2$ (C, H, N).

5.1.22. (R)-3-(4-Methyl-4,5-dihydrooxazol-2-yl)phenyl cyclohexyl-carbamate (**5b**)

White crystals (46 mg, 27%): mp. 133–134 °C; R_f (50% EtOAc in hex) 0.24; $[\alpha]_D$ 45 (c = 0.5, CDCl_3); ^1H NMR (CDCl_3) 7.77 (d, 1H, J = 7.7 Hz), 7.70 (m, 1H), 7.38 (t, 1H, J = 7.9 Hz), 7.24 (dd, 1H, J = 8.1, 1.4 Hz), 4.94 (d, 1H, J = 7.4 Hz), 4.51 (dd, 1H, J = 9.3, 8.1 Hz), 4.42–4.32 (m, 1H), 3.94 (t, 1H, J = 7.9 Hz), 3.60–3.50 (m, 1H), 2.07–1.96 (m, 2H), 1.78–1.70 (m, 2H), 1.66–1.57 (m, 1H), 1.43–1.32 (m, 2H), 1.35 (d, 3H, J = 6.6 Hz), 1.27–1.15 (m, 3H); ^{13}C NMR (CDCl_3) 162.8, 153.4, 151.0, 129.1 (2C), 124.9, 124.6, 121.6, 74.1, 62.0, 50.1, 33.2, 25.4, 24.7, 21.4; Rt 22 min, 99 ee-%; Anal. $\text{C}_{17}\text{H}_{22}\text{N}_2\text{O}_3$ (C, H, N).

5.1.23. (S)-3-(4-Benzyl-4,5-dihydrooxazol-2-yl)phenol (**18c**)

White waxy solid (446 mg, 52%): mp. 109–111 °C; R_f (10% Et_2O in CH_2Cl_2) 0.14; $[\alpha]_D$ 39 (c = 0.5, CHCl_3); ^1H NMR (CDCl_3) 7.92 (s, 1H),

7.50 (dd, 1H, J = 2.4, 1.5 Hz), 7.39 (td, 1H, J = 7.7, 1.2 Hz), 7.30–7.18 (m, 6H), 6.98 (ddd, 1H, J = 8.1, 2.6, 1.0 Hz), 4.65–4.57 (m, 1H), 4.35 (t, 1H, J = 9.0 Hz), 4.17 (dd, 1H, J = 8.6, 7.2 Hz), 3.23 (dd, 1H, J = 13.7, 4.9 Hz), 2.75 (dd, 1H, J = 13.7, 9.0 Hz); ^{13}C NMR (CDCl_3) 164.8, 156.4, 137.6, 129.7, 129.3, 128.6, 128.3, 126.6, 120.2, 119.4, 115.2, 72.0, 67.2, 41.5; Anal. $\text{C}_{16}\text{H}_{15}\text{NO}_2$ (C, H, N).

5.1.24. (S)-3-(4-Benzyl-4,5-dihydrooxazol-2-yl)phenyl cyclohexyl-carbamate (**5c**)

White crystals (120 mg, 56%): mp. 152–155 °C; R_f 0.46 (10% Et_2O in CH_2Cl_2); $[\alpha]_D$ 5.8 (c = 0.5, CHCl_3); ^1H NMR (CDCl_3) 7.78 (d, 1H, J = 7.8 Hz), 7.70 (t, 1H, J = 1.8 Hz), 7.39 (t, 1H, J = 8.0 Hz), 7.33–7.21 (m, 6H), 4.93 (d, 1H, J = 7.6 Hz), 4.62–4.54 (m, 1H), 4.34 (t, 1H, J = 8.9 Hz), 4.13 (dd, 1H, J = 8.3, 7.5 Hz), 3.61–3.51 (m, 1H), 3.23 (dd, 1H, J = 13.7, 5.1 Hz), 2.72 (dd, 1H, J = 13.7, 8.9 Hz), 2.05–1.97 (m, 2H), 1.78–1.70 (m, 2H), 1.66–1.61 (m, 1H), 1.43–1.32 (m, 2H), 1.28–1.14 (m, 3H); ^{13}C NMR (CDCl_3) 163.3, 153.3, 151.0, 137.9, 129.2, 129.2, 129.0, 128.6, 126.5, 125.0, 124.7, 121.6, 71.9, 67.9, 50.2, 41.8, 33.2, 25.4, 24.7; Rt 57 min, 98 ee-%; Anal. $\text{C}_{23}\text{H}_{26}\text{N}_2\text{O}_3$ (C, H, N).

5.1.25. (R)-3-(4-Benzyl-4,5-dihydrooxazol-2-yl)phenol (**18d**)

White waxy solid (267 mg, 41%): mp. 108–111 °C; R_f 0.21 (15% Et_2O in CH_2Cl_2); $[\alpha]_D$ –40 (c = 0.5, CHCl_3); ^1H NMR (CDCl_3) 8.50 (br s, 1H), 7.50 (dd, 1H, J = 2.3, 1.5 Hz), 7.36 (td, 1H, J = 7.7, 1.1 Hz), 7.29–7.18 (m, 6H), 6.97 (ddd, 1H, J = 8.2, 2.5, 0.9 Hz), 4.66–4.57 (m, 1H), 4.34 (t, 1H, J = 9.0 Hz), 4.17 (dd, 1H, J = 8.5, 7.3 Hz), 3.24 (dd, 1H, J = 13.7, 4.8 Hz), 2.75 (dd, 1H, J = 13.7, 9.2 Hz); ^{13}C NMR (CDCl_3) 165.0, 156.6, 137.5, 129.7, 129.3, 128.6, 128.2, 126.6, 120.1, 119.5, 115.2, 72.0, 67.0, 41.4; Anal. $\text{C}_{16}\text{H}_{15}\text{NO}_2$ (C, H, N).

5.1.26. (R)-3-(4-Benzyl-4,5-dihydrooxazol-2-yl)phenyl cyclohexyl-carbamate (**5d**)

White crystals (152 mg, 57%): mp. 153–155 °C; R_f 0.38 (13% Et_2O in CH_2Cl_2); $[\alpha]_D$ –7.4 (c = 0.5, CHCl_3); ^1H NMR (CDCl_3) 7.78 (d, 1H, J = 7.7 Hz), 7.7 (m, 1H), 7.39 (t, 1H, J = 8.0 Hz), 7.33–7.20 (m, 6H), 4.93 (d, 1H, J = 8.0 Hz), 4.62–4.53 (m, 1H), 4.33 (t, 1H, J = 8.9 Hz), 4.13 (dd, 1H, J = 8.3, 7.5 Hz), 3.62–3.50 (m, 1H), 3.23 (dd, 1H, J = 13.7, 5.1 Hz), 2.71 (dd, 1H, J = 13.7, 8.9 Hz), 2.05–1.97 (m, 2H), 1.77–1.70 (m, 2H), 1.66–1.58 (m, 1H), 1.43–1.32 (m, 2H), 1.28–1.14 (m, 3H); ^{13}C NMR (CDCl_3) 163.3, 153.3, 151.0, 137.9, 129.2, 129.2, 129.0, 128.5, 126.5, 125.0, 124.7, 121.6, 71.9, 67.9, 50.1, 41.8, 33.2, 25.4, 24.7; Rt 22 min, 99 ee-%; Anal. $\text{C}_{23}\text{H}_{26}\text{N}_2\text{O}_3$ (C, H, N).

5.1.27. (S)-3-(4-((1H-Indol-3-yl)methyl)-4,5-dihydrooxazol-2-yl)-phenol (**18e**)

Gray powder (140 mg, 35%): mp. 183–186 °C; R_f (50% EtOAc in hex) 0.20; $[\alpha]_D$ 59 (c = 0.3, MeOH); ^1H NMR ($\text{DMSO}-d_6$) 10.85 (br s, 1H), 9.68 (s, 1H), 7.59 (d, 1H, J = 7.9 Hz), 7.33 (d, 1H, J = 8.0 Hz), 7.31–7.19 (m, 4H), 7.06 (td, 1H, J = 7.5, 1.1 Hz), 6.98 (td, 1H, J = 7.4, 1.0 Hz), 6.93–6.89 (m, 1H), 4.64–4.55 (m, 1H), 4.38 (dd, 1H, J = 9.4, 8.4 Hz), 4.07 (t, 1H, J = 7.9 Hz), 3.13 (dd, 1H, J = 14.8, 4.9 Hz), 2.82 (dd, 1H, J = 14.6, 8.1 Hz); ^{13}C NMR ($\text{DMSO}-d_6$) 162.1, 157.3, 136.1, 129.6, 128.8, 127.5, 123.4, 120.9, 118.5, 118.5, 118.4, 118.3, 114.4, 111.3, 110.4, 71.7, 66.6, 31.0; Anal. $\text{C}_{18}\text{H}_{16}\text{N}_2\text{O}_2$ (C, H, N).

5.1.28. (S)-3-(4-((1H-Indol-3-yl)methyl)-4,5-dihydrooxazol-2-yl)-phenyl cyclohexylcarbamate (**7**)

White crystals (35 mg, 35%): mp. 149–151 °C; R_f 0.23 (10% Et_2O in CH_2Cl_2); $[\alpha]_D$ 22 (c = 0.5, CDCl_3); ^1H NMR (CDCl_3) 8.11 (br s, 1H), 7.79 (d, 1H, J = 7.8 Hz), 7.72 (s, 1H), 7.66 (d, 1H, J = 7.8 Hz), 7.41–7.33 (m, 2H), 7.20 (td, 1H, J = 7.5, 1.1 Hz), 7.13 (td, 1H, J = 7.4, 1.0 Hz), 7.28–7.24 (m, 1H), 7.04 (d, 1H, J = 2.2 Hz), 4.94 (d, 1H, J = 7.8 Hz), 4.75–4.67 (m, 1H), 4.33 (t, 1H, J = 8.9 Hz), 4.15 (t, 1H, J = 7.9 Hz), 3.62–3.51 (m, 1H), 3.36 (dd, 1H, J = 14.5, 4.6 Hz), 2.88 (dd, 1H, J = 14.6, 8.9 Hz), 2.05–1.97 (m, 2H), 1.78–1.70 (m, 2H), 1.67–1.58 (m, 1H), 1.43–1.32

(m, 2H), 1.28–1.14 (m, 3 H); ^{13}C NMR (CDCl_3) 163.2, 153.4, 151.0, 136.2, 129.2 (2C), 127.7, 125.0, 124.6, 122.4, 122.1, 121.6, 119.5, 118.8, 112.0, 111.1, 72.3, 67.0, 50.2, 33.2, 31.3, 25.4, 24.7; Anal. $\text{C}_{25}\text{H}_{27}\text{N}_3\text{O}_3$ (C, H, N).

5.1.29. Procedure for preparation of **19a–d**

Et_3N was used only in the case of **19a–b**.

5.1.29.1. (R)-Methyl 2-(3-hydroxyphenyl)-4,5-dihydrooxazole-4-carboxylate (19a). To a mixture of 3-cyanophenol (1840 mg, 15.5 mmol, 100 mol-%) in dry CH_2Cl_2 (36 mL) was added dry MeOH (3.2 mL, 79 mmol, 510 mol-%) and the mixture was bubbled with HCl gas in an ice bath. The mixture was stirred at 2 °C for 3 days and solvents were evaporated. Filtering and washing with dry Et_2O gave methyl 3-hydroxybenzimidate hydrochloride (2.67 g, 92%) as a white powder: ^1H NMR ($\text{DMSO}-d_6$) 11.68 (br s, 1H), 10.34 (s, 1H), 7.57–7.53 (m, 1H), 7.46–7.41 (m, 2H), 7.24–7.21 (m, 1H), 4.27 (s, 3H). (R)-Serine methyl ester hydrochloride (125 mg, 0.80 mmol, 100 mol-%) was suspended in dry CH_2Cl_2 and Et_3N was added (180 μL , 1.28 mmol, 160 mol-%) followed by above described imidate salt (153 mg, 0.82 mmol, 100 mol-%) and the mixture was refluxed overnight. Solvent was evaporated and remaining solid partitioned between H_2O (10 mL) and EtOAc (15 mL). Organic phase was washed with H_2O (10 mL). Aqueous phases were combined and backwashed with EtOAc (2 \times 15 mL). Organic phases were combined, washed with brine (20 mL), dried over Na_2SO_4 , filtered and evaporated. Purification by FC (twice, 70% EtOAc:hex, then 5% MeOH: CH_2Cl_2) gave **19a** (122 mg, 68%) as an oil: R_f (70% EtOAc:hex) 0.33; $[\alpha]_D^{20}$ –57 (c = 1, CDCl_3); ^1H NMR (CDCl_3) 8.57 (s, 1H), 7.42 (dd, 1H, J = 2.4, 1.6 Hz), 7.38 (app. ddd, 1H), 7.18 (t, 1H, J = 7.9 Hz), 6.96 (ddd, 1H, J = 8.2, 2.5, 0.9 Hz), 4.96 (dd, 1H, J = 10.7, 7.8 Hz), 4.69 (dd, 1H, J = 8.7, 7.9 Hz), 4.58 (dd, 1H, J = 10.7, 8.8 Hz), 3.69 (s, 3H); ^{13}C NMR (CDCl_3) 171.3, 167.1, 156.6, 129.6, 127.2, 120.3, 119.8, 115.4, 69.6, 67.7, 52.7; HRMS (ESI) calcd for $[\text{M} + \text{H}]^+$ $\text{C}_{11}\text{H}_{11}\text{NO}_4$: 222.0766, found 222.0766.

5.1.30. (R)-Methyl 2-(3-(cyclohexylcarbamoyloxy)phenyl)-4,5-dihydrooxazole-4-carboxylate (5e)

White crystals (136 mg, 73%): mp. 114–116 °C; R_f (17% Et_2O in CH_2Cl_2) 0.33; $[\alpha]_D^{20}$ –68 (c = 0.5, CHCl_3); ^1H NMR (CDCl_3) 7.81 (d, 1H, J = 7.8 Hz), 7.75 (s, 1H), 7.39 (t, 1H, J = 8.0 Hz), 7.29–7.26 (m, 1H), 4.95 (dd, 2H, J = 10.5, 8.0 Hz), 4.69 (t, 1H, J = 8.3 Hz), 4.59 (dd, 1H, J = 10.5, 8.8 Hz), 3.82 (s, 3H), 3.60–3.51 (m, 1H), 2.04–1.97 (m, 2H), 1.78–1.70 (m, 2H), 1.67–1.59 (m, 1H), 1.43–1.32 (m, 2H), 1.27–1.16 (m, 3H); ^{13}C NMR (CDCl_3) 171.4, 165.6, 153.3, 151.0, 129.2, 128.1, 125.3, 125.2, 121.9, 69.6, 68.6, 52.7, 50.1, 33.2, 25.4, 24.7; Rt 99 min, 96 ee-%; Anal. $\text{C}_{18}\text{H}_{22}\text{N}_2\text{O}_5$ (C, H, N).

5.1.31. (S)-Methyl 2-(3-hydroxyphenyl)-4,5-dihydrooxazole-4-carboxylate (19b)

Colourless oil (122 mg, 68%): R_f (60% EtOAc in hex) 0.28; $[\alpha]_D^{20}$ 65 (c = 1.8, CDCl_3); ^1H NMR (CDCl_3) 8.16 (s, 1H), 7.43–7.42 (m, 1H), 7.40 (d, 1H, J = 7.8 Hz), 7.20 (t, 1H, J = 7.9 Hz), 6.97 (ddd, 1H, J = 8.2, 2.5, 0.9 Hz), 4.96 (dd, 1H, J = 10.7, 7.9 Hz), 4.69 (dd, 1H, J = 8.7, 7.9 Hz), 4.59 (dd, 1H, J = 10.7, 8.8 Hz), 3.71 (s, 3H); ^{13}C NMR (CDCl_3) 171.4, 170.0, 156.5, 129.6, 127.3, 120.4, 119.8, 115.4, 69.6, 67.8, 52.7; HRMS (ESI) calcd for $[\text{M} + \text{H}]^+$ $\text{C}_{11}\text{H}_{11}\text{NO}_4$: 222.0766, found 222.0759.

5.1.32. (S)-Methyl 2-(3-(cyclohexylcarbamoyloxy)phenyl)-4,5-dihydrooxazole-4-carboxylate (5f)

White crystals (141 mg, 75%): mp. 114–116 °C; R_f (17% Et_2O : CH_2Cl_2) 0.33; $[\alpha]_D^{20}$ 73 (c = 0.5, CHCl_3); ^1H NMR (CDCl_3) 7.81 (d, 1H, J = 7.8 Hz), 7.75 (s, 1H), 7.39 (t, 1H, J = 7.9 Hz), 7.29–7.26 (m, 1H), 4.94 (dd, 2H, J = 10.5, 8.0 Hz), 4.69 (t, 1H, J = 7.8 Hz), 4.59 (dd, 1H,

J = 10.6, 8.8 Hz), 3.82 (s, 3H), 3.59–3.52 (m, 1H), 2.04–1.97 (m, 2H), 1.78–1.70 (m, 2H), 1.67–1.59 (m, 1H), 1.43–1.32 (m, 2H), 1.27–1.16 (m, 3H); ^{13}C NMR (CDCl_3) 171.4, 165.6, 153.3, 151.0, 129.2, 128.1, 125.3, 125.2, 121.9, 69.6, 68.6, 52.7, 50.1, 33.2, 25.4, 24.7; Rt 34 min, 97 ee-%; Anal. $\text{C}_{17}\text{H}_{22}\text{N}_2\text{O}_3$ (C, H, N).

5.1.33. (R)-3-(5-Methyl-4,5-dihydrooxazol-2-yl)phenol (19c)

White crystals (137 mg, 26%): R_f (EtOAc) 0.33; $[\alpha]_D^{20}$ –4.5 (c = 1.0, CDCl_3); ^1H NMR (CDCl_3) 9.64 (br s, 1H), 7.48–7.46 (app. dd, 1H), 7.34–7.30 (m, 1H), 7.19 (t, 1H, J = 7.9 Hz), 6.95 (ddd, 1H, J = 8.1, 2.5, 0.9 Hz), 4.91–4.81 (m, 1H), 4.13 (dd, 1H, J = 14.2, 9.5 Hz), 4.58 (dd, 1H, J = 14.2, 7.6 Hz), 1.42 (d, 3H, J = 6.2 Hz); ^{13}C NMR (CDCl_3) 165.1, 157.0, 129.6, 128.2, 119.7, 119.5, 115.1, 76.6, 60.3, 20.9; Rt 15 min, 99 ee-%; Anal. $\text{C}_{10}\text{H}_{11}\text{NO}_2$ (C, H, N).

5.1.34. (R)-3-(5-Methyl-4,5-dihydrooxazol-2-yl)phenyl cyclohexylcarbamate (6a)

White crystals (75 mg, 54%): mp. 141–142 °C; R_f (20% acetone in CH_2Cl_2) 0.7; $[\alpha]_D^{20}$ –8.9 (c = 0.9, CDCl_3); ^1H NMR (CDCl_3) 7.77 (d, 1H, J = 7.7 Hz), 7.71–7.68 (m, 1H), 7.38 (t, 1H, J = 7.9 Hz), 7.26–7.22 (app. dd, 1H), 4.98 (br d, 1H, J = 7.6 Hz), 4.89–4.79 (m, 1H), 4.14 (dd, 1H, J = 14.6, 9.4 Hz), 3.60 (dd, 1H, J = 14.5, 7.4 Hz), 3.60–3.50 (m, 1H), 2.08–1.96 (m, 2H), 1.81–1.69 (m, 2H), 1.67–1.58 (m, 1H), 1.45–1.31 (m, 2H), 1.41 (t, 3H, J = 6.2 Hz) 1.29–1.13 (m, 3H); ^{13}C NMR (CDCl_3) 163.2, 153.4, 151.0, 129.3, 129.1, 124.8, 124.5, 121.4, 76.4, 61.6, 50.1, 33.2, 25.4, 24.7, 21.1; Rt 64 min, 99 ee-%; Anal. $\text{C}_{17}\text{H}_{22}\text{N}_2\text{O}_3$ (C, H, N).

5.1.35. (S)-3-(5-Methyl-4,5-dihydrooxazol-2-yl)phenol (19d)

White crystals (126 mg, 71%): mp. 104–106 °C; R_f (EtOAc) 0.33; $[\alpha]_D^{20}$ 3.7 (c = 1.0, CDCl_3); ^1H NMR (CDCl_3) 9.63 (br s, 1H), 7.48–7.46 (app. dd, 1H), 7.34–7.30 (m, 1H), 7.19 (t, 1H, J = 7.9 Hz), 6.95 (ddd, 1H, J = 8.1, 2.5, 0.9 Hz), 4.91–4.81 (m, 1H), 4.13 (dd, 1H, J = 14.2, 9.5 Hz), 4.58 (dd, 1H, J = 14.2, 7.6 Hz), 1.42 (d, 3H, J = 6.2 Hz); ^{13}C NMR (CDCl_3) 165.1, 157.0, 129.6, 128.2, 119.7, 119.5, 115.1, 76.6, 60.3, 20.9; Rt 10.8 min, 99 ee-%; Anal. $\text{C}_{10}\text{H}_{11}\text{NO}_2$ (C, H, N).

5.1.36. (S)-3-(5-Methyl-4,5-dihydrooxazol-2-yl)phenyl cyclohexylcarbamate (6b)

White crystals (98 mg, 58%): mp. 140–142 °C; R_f (20% acetone in CH_2Cl_2) 0.7; $[\alpha]_D^{20}$ 9.3 (c = 1.0, CDCl_3); ^1H NMR (CDCl_3) 7.77 (d, 1H, J = 7.7 Hz), 7.70–7.68 (m, 1H), 7.38 (t, 1H, J = 7.9 Hz), 7.26–7.22 (app. dd, 1H), 4.98 (br d, 1H, J = 7.6 Hz), 4.89–4.79 (m, 1H), 4.14 (dd, 1H, J = 14.6, 9.4 Hz), 3.60 (dd, 1H, J = 14.5, 7.4 Hz), 3.60–3.50 (m, 1H), 2.08–1.96 (m, 2H), 1.81–1.69 (m, 2H), 1.67–1.58 (m, 1H), 1.45–1.31 (m, 2H), 1.41 (t, 3H, J = 6.2 Hz) 1.29–1.13 (m, 3H); ^{13}C NMR (CDCl_3) 163.2, 153.4, 151.0, 129.3, 129.1, 124.8, 124.5, 121.4, 76.4, 61.6, 50.1, 33.2, 25.4, 24.7, 21.1; Rt 23.5 min, 97 ee-%; Anal. $\text{C}_{17}\text{H}_{22}\text{N}_2\text{O}_3$ (C, H, N).

5.2. Biological testing protocols

5.2.1. Animals and preparation of rat brain homogenate for FAAH assay

Eight-week-old male Wistar rats were used in these studies. All animal experiments were approved by the local ethics committee. The animals lived in a 12-h light/12-h dark cycle (lights on at 0700 h) with water and food available *ad libitum*.

The rats were decapitated, whole brains minus cerebellum were dissected and homogenized in one volume (v/w) of ice-cold 0.1 M potassium phosphate buffer (pH 7.4) with a Potter–Elvehjem homogenizer (Heidolph). The homogenate was centrifuged at 10,000g for 20 min at 4 °C and the resulting supernatant was used as a source of FAAH activity. The protein concentration of the supernatant (7.2 mg/mL) was determined by the method of Bradford with BSA as the standard [59]. Aliquots of the supernatant were stored at –80 °C until use.

5.2.2. Animals and preparation of rat cerebellar membranes for MGL assay

Four-week-old male Wistar rats were used in these studies. All animal experiments were approved by the local ethics committee. The animals lived in a 12-h light/12-h dark cycle (lights on at 0700 h), with water and food available *ad libitum*. The rats were decapitated, 8 h after lights on (1500 h), whole brains were removed, dipped in isopentane on dry ice and stored at -80°C . Membranes were prepared as previously described [60–62].

Briefly, cerebella (minus brain stem) from eight animals were weighed and homogenized in nine volumes of ice-cold 0.32 M sucrose with a glass Teflon homogenizer. The crude homogenate was centrifuged at low speed (1000g for 10 min at 4°C) and the pellet was discharged. The supernatant was centrifuged at high speed (100,000g for 10 min at 4°C). The pellet was resuspended in ice-cold deionized water and washed twice, repeating the high-speed centrifugation. Finally, membranes were resuspended in 50 mM Tris–HCl, pH 7.4 with 1 mM EDTA and aliquoted for storage at -80°C . The protein concentration of the final preparation, measured by the Bradford method [59], was 11 mg/mL.

5.2.3. In vitro assay for FAAH activity

The assay for FAAH activity has been described previously [63]. The endpoint enzymatic assay was developed to quantify FAAH activity with tritium-labelled arachidonylethanolamide (ethanolamine $1\text{-}^3\text{H}$). The assay buffer used was 0.1 M potassium phosphate (pH 7.4) and test compounds were dissolved in DMSO (the final DMSO concentration was max 5% v/v). The incubations were performed in the presence of 0.5% (w/v) BSA (essentially fatty acid free). Test compounds were preincubated with rat brain homogenate protein (18 μg) for 10 min at 37°C (60 μL). At the 10 min time point, arachidonylethanolamide was added so that its final concentration was 2 μM (containing 50×10^{-3} μCi of 60 Ci/mmol [^3H]AEA) and the final incubation volume was 100 μL . The incubations proceeded for 10 min at 37°C . EtOAc (400 μL) was added at the 20 min time point to stop the enzymatic reaction. Additionally, 100 μL of unlabelled ethanolamine (1 mM) was added as a ‘carrier’ for radioactive ethanolamine. Samples were centrifuged at 16,000g for 4 min at rt, and aliquots (100 μL) from aqueous phase containing [ethanolamine $1\text{-}^3\text{H}$] were measured for radioactivity by liquid scintillation counting (Wallac 1450 MicroBeta; Wallac Oy, Finland).

5.2.4. In vitro assay for MGL activity in rat cerebellar membranes

The assay for MGL activity has been described previously [64]. Briefly, experiments were carried out with preincubations (80 μL , 30 min at 25°C) containing 10 μg membrane protein, 44 mM Tris–HCl (pH 7.4), 0.9 mM EDTA, 0.5% (wt/vol) BSA and 1.25% (vol/vol) DMSO as a solvent for inhibitors. The preincubated membranes were kept at 0°C just prior to the experiments. The incubations (90 min at 25°C) were initiated by adding 40 μL of preincubated membrane cocktail, in a final volume of 400 μL . The final volume contained 5 μg membrane protein, 54 mM Tris–HCl (pH 7.4), 1.1 mM EDTA, 100 mM NaCl, 5 mM MgCl_2 , 0.5% (wt/vol) BSA and 50 μM of 2-AG. At time points of 0 and 90 min, 100- μL samples were removed from the incubation, acetonitrile (200 μL) was added to stop the enzymatic reaction and the pH of the samples was simultaneously decreased to 3.0 with phosphoric acid (added to acetonitrile) to stabilize 2-AG against acyl migration to 1(3)-AG. Samples were centrifuged at 23,700g for 4 min at rt prior to HPLC analysis of the supernatant.

5.2.5. HPLC method

The analytical HPLC was performed as previously described [17]. Briefly, the analytical HPLC system consisted of a Merck Hitachi (Hitachi Ltd., Tokyo, Japan) L-7100 pump, D-7000 interface module,

L-7455 diode-array UV detector (190–800 nm, set at 211 nm) and L-7250 programmable autosampler. The separations were accomplished on a Zorbax SB-C18 endcapped reversed-phase precolumn (4.6×12.5 mm, 5 μm) and column (4.6×150 mm, 5 μm) (Agilent, USA). The injection volume was 50 μL . A mobile phase mixture of 28% phosphate buffer (30 mM, pH 3.0) in acetonitrile was used at a flow rate of 2.0 mL/min. Retention times were 5.8 min for 2-AG, 6.3 min for 1(3)-AG and 10.2 min for arachidonic acid. The relative concentrations of 2-AG, 1(3)-AG and arachidonic acid were determined by the corresponding peak areas. This was justified by the equivalence of response factors for the studied compounds, and was supported by the observation that the sum of the peak areas was constant throughout the experiments.

5.2.6. Human recombinant MGL assay

The endpoint enzymatic assay was developed to quantify human recombinant MGL (Cayman Chemical, cat# 10008354) activity with tritium-labelled 2-oleoylglycerol (2-OG) [glycerol-1,2,3- ^3H] (American Radiolabeled Chemicals Inc., St Louis, MO, USA). The assay buffer was 50 mM Tris–HCl, pH 7.4; 1 mM EDTA and test compounds were dissolved in DMSO (the final DMSO concentration was not more than 5% v/v). The incubations were performed in the presence of 0.5% (w/v) BSA (essentially fatty acid free). hrMGL was preincubated with test compounds for 10 min at 37°C (60 μL). At the 10 min time point, 2-OG was added to achieve the final concentration of 50 μM (containing 112×10^{-3} μCi of 40 Ci/mmol [^3H]2-OG) with the final incubation volume of 100 μL . The incubations proceeded for 10 min at 37°C . EtOAc (400 μL) was added at the 20 min time point to stop the enzymatic reaction. Additionally, 100 μL of buffer (50 mM Tris–HCl, pH 7.4; 1 mM EDTA) was added. The samples were centrifuged at 16,000g for 4 min at rt, and aliquots (100 μL) were taken from the aqueous phase, which contained glycerol-1,2,3- ^3H , and measured for radioactivity by liquid scintillation counting (Wallac 1450 MicroBeta; Wallac Oy, Finland).

5.2.7. Data analyses

The results from the enzyme inhibition experiments are presented as mean \pm 95% confidence intervals of at least three independent experiments performed in duplicate. Data analyses for the dose–response curves were calculated as non-linear regressions using GraphPad Prism 4.0 for Windows.

5.3. Molecular modelling

5.3.1. Structure construction

The 3-D coordinates in the X-ray crystal structure of murine FAAH in complex with covalently bound inhibitor methyl arachidonyl fluorophosphonate (MAFP) (Protein Data Bank code 1MT5, resolution 2.8 Å) [42] was used as an enzyme model for the docking calculations. Missing side chain atoms were added into the FAAH monomer (chain A extracted from the X-ray data) of the crystal structure by using Lovell rotamer library [65] and optimized in polarizable AMBER07_FF02 force field [66] (energy gradient of 0.01 kcal/mol) while keeping the rest of the protein atoms fixed, as implemented in Sybyl 8.1 [67]. Hydrogen atoms were added with MolProbity (v.3.15) [68] server by allowing the program to optimize hydrogen bonding by flipping Asn, Gln or His, where applicable. The orientation of the hydrogen atoms of the catalytic region amino acids (catalytic triad) [42,69] was inspected to ensure that a hydrogen bond was formed between hydroxyl groups of Ser217 and Ser241 and one between side chain of Ser217 and side chain of Lys142.

The 3-D coordinates of the ligands were generated in Sybyl 8.1 following an energy minimization to energy gradient of 0.005 kcal/mol in Merck molecular force field (MMFF94s) [70] with Powell conjugate gradient method.

5.3.2. Molecular docking

Version 4.0 of GOLD [43] was used as a docking tool in this study. The binding site of FAAH was defined to range 15 Å radius from the oxygen atom of catalytic Ser241 side chain hydroxyl group (with 'detect cavity' feature of GOLD toggled on). The default GoldScore empirical fitness function was used as a scoring function for the generated poses. In order to maximize the conformational space sampled during the docking calculations, a preset '200% efficiency' setting was utilized for 1000 separate genetic algorithm (GA) docking runs for each ligand. To ensure that different possible binding modes are inspected upon visualization of the results, and not only the top-ranking poses, RMSD-based complete linkage clustering was applied. Clustering distance of 1.0 Å (as implemented in GOLD) was used to derive the clusters of poses. The top-ranking (according to GOLD) poses of three most abundant clusters, in terms of cluster members, were visualized for each ligand. The highest scoring pose of the most abundant cluster was considered for the further analyses.

5.3.3. GRID interaction fields

In order to analyze and identify possible hot spots for favorable protein–ligand interactions in the FAAH active site and consequently shed light on the measured enantioselectivity, GRID [46] molecular interaction field (MIF) analysis was carried out. For GRID calculations, the active site of the modified FAAH structure (see Section 5.3.1) was enclosed in a $26 \times 26 \times 25$ Å box with grid spacing of 0.2 Å. Only lone pairs and tautomeric hydrogens were allowed to alter in response to the probes (directive MOVE = 0). To reflect the oxazoline ring and its different substituents found in the enantiomeric pairs, the following GRID probes were used in this study: methyl (C3), sp^2 aromatic carbon (C1=), sp^2 nitrogen with a lone pair (N:), sp^2 carbonyl oxygen (O), and aromatic/aliphatic ether oxygen (OC1). The resulting MIFs were visually analyzed.

5.3.4. Electrostatic potential

To briefly explore the nucleophilic characteristics of the chiral carbamates, we calculated the electrostatic potential $V(r)$ of the enantiomers. Starting from the docked conformations, the molecules were optimized and $V(r)$ was calculated in Hartree-Fock/6-311G** level of theory with Gaussian 03 [71]. The $V(r)$ isosurfaces were visualized with VMD 1.8.6 [72].

Acknowledgments

We thank Ms Anna Minkkilä for help in biological testing. The National Technology Agency of Finland, The National Graduate School in Informational and Structural Biology (ISB), and Finnish Cultural Foundation are greatly acknowledged for financial support.

Appendix

Analysis data of novel compounds.

Compound	Formula	Calculated	Found
2a	C ₁₇ H ₁₆ N ₂ O ₃	C, 68.91; H, 5.44; N, 9.45	C, 68.84; H, 5.37; N, 9.44
2b	C ₁₆ H ₁₅ N ₃ O ₃	C, 64.64; H, 5.09; N, 14.13	C, 64.61; H, 4.81; N, 14.13
15	C ₁₁ H ₇ N ₃ O ₂	M + Na ⁺ = 236.0436	HRMS (ESI) <i>m/z</i> 236.0447
2c	C ₁₅ H ₁₄ N ₄ O ₃	C, 60.40; H, 4.73; N, 18.78	C, 60.09; H, 4.58; N, 18.21
	C ₁₅ H ₁₄ N ₄ O ₃	M + Na ⁺ = 321.0964	HRMS (ESI) <i>m/z</i> 321.0951
3a	C ₁₃ H ₁₆ N ₂ O ₃	C, 62.89; H, 6.50; N, 11.28	C, 62.77; H, 6.26; N, 11.15
3b	C ₁₅ H ₁₈ N ₂ O ₃	C, 65.68; H, 6.61; N, 10.21	C, 65.62; H, 6.91; N, 10.20
3c	C ₁₆ H ₂₀ N ₂ O ₃	C, 66.65; H, 6.99; N, 9.72	C, 66.79; H, 7.13; N, 9.61
4a	C ₁₇ H ₂₂ N ₂ O ₃	C, 67.53; H, 7.33; N, 9.26	C, 67.35; H, 7.40; N, 9.38
4b	C ₁₈ H ₂₄ N ₂ O ₃	C, 68.33; H, 7.65; N, 8.85	C, 68.33; H, 7.92; N, 8.77
18a	C ₁₀ H ₁₁ NO ₂	C, 67.78; H, 6.26; N, 7.90	C, 67.88; H, 5.85; N, 7.72

Appendix (continued)

Compound	Formula	Calculated	Found
4c	C ₁₆ H ₂₀ N ₂ O ₃	C, 66.65; H, 6.99; N, 9.72	C, 66.68; H, 7.15; N, 9.82
5a	C ₁₇ H ₂₂ N ₂ O ₃	C, 67.53; H, 7.33; N, 9.26	C, 67.77; H, 7.26; N, 9.09
18b	C ₁₀ H ₁₁ NO ₂	C, 67.78; H, 6.26; N, 7.90	C, 67.89; H, 6.10; N, 7.90
5b	C ₁₇ H ₂₂ N ₂ O ₃	C, 67.53; H, 7.33; N, 9.26	C, 67.63; H, 7.33; N, 9.17
18c	C ₁₆ H ₁₅ NO ₂	C, 75.87; H, 5.97; N, 5.53	C, 75.79; H, 5.74; N, 5.50
5c	C ₂₃ H ₂₆ N ₂ O ₃	C, 72.99; H, 6.92; N, 7.40	C, 73.17; H, 6.70; N, 7.37
18d	C ₁₆ H ₁₅ NO ₂	C, 75.87; H, 5.97; N, 5.53	C, 75.96; H, 5.71; N, 5.25
5d	C ₂₃ H ₂₆ N ₂ O ₃	C, 72.99; H, 6.92; N, 7.40	C, 73.09; H, 7.09; N, 7.44
19a	C ₁₁ H ₁₁ NO ₄	M + H ⁺ = 222.0766	HRMS (ESI) <i>m/z</i> 222.0766
5e	C ₁₈ H ₂₂ N ₂ O ₅	C, 62.42; H, 6.40; N, 8.09	C, 62.47; H, 6.15; N, 8.03
19b	C ₁₁ H ₁₁ NO ₄	M + H ⁺ = 222.0766	HRMS (ESI) <i>m/z</i> 222.0759
5f	C ₁₈ H ₂₂ N ₂ O ₅	C, 62.42; H, 6.40; N, 8.09	C, 62.45; H, 6.12; N, 8.02
19c	C ₁₀ H ₁₁ NO ₂	C, 67.78; H, 6.26; N, 7.90	C, 67.52; H, 6.23; N, 8.10
6a	C ₁₇ H ₂₂ N ₂ O ₃	C, 67.53; H, 7.33; N, 9.26	C, 67.35; H, 7.30; N, 9.40
19d	C ₁₀ H ₁₁ NO ₂	C, 67.78; H, 6.26; N, 7.90	C, 67.58; H, 6.23; N, 8.05
6b	C ₁₇ H ₂₂ N ₂ O ₃	C, 67.53; H, 7.33; N, 9.26	C, 67.30; H, 7.28; N, 9.42
18e	C ₁₈ H ₁₆ N ₂ O ₂	C, 73.95; H, 5.52; N, 9.58	C, 73.60; H, 5.43; N, 9.39
7	C ₂₅ H ₂₇ N ₃ O ₃	C, 71.92; H, 6.52; N, 10.06	C, 71.58; H, 6.32; N, 10.05

References

- [1] W.A. Devane, L. Hanus, A. Breuer, R.G. Pertwee, L.A. Stevenson, G. Griffin, D. Gibson, A. Mandelbaum, A. Etinger, R. Mechoulam, *Science* 258 (1992) 1946–1949.
- [2] R. Mechoulam, S. Ben-Shabat, L. Hanus, M. Ligumsky, N.E. Kaminski, A.R. Schatz, A. Gopher, S. Almog, B.R. Martin, D.R. Compton, R.G. Pertwee, G. Griffin, M. Bayewitch, J. Barg, Z. Vogel, *Biochem. Pharmacol.* 50 (1995) 83–90.
- [3] T. Sugiura, S. Kondo, A. Sukagawa, S. Nakane, A. Shinoda, K. Itoh, A. Yamashita, K. Waku, *Biochem. Biophys. Res. Commun.* 215 (1995) 89–97.
- [4] V. Di Marzo, M. Bifulco, L. De Petrocellis, *Nat. Rev. Drug Discov.* 3 (2004) 771–784.
- [5] D.M. Lambert, C.J. Fowler, *J. Med. Chem.* 48 (2005) 5059–5087.
- [6] J.M. Walker, S.M. Huang, N.M. Strangman, K. Tsou, M.C. Sañudo-Peña, *Proc. Natl. Acad. Sci. U.S.A.* 96 (1999) 12198–12203.
- [7] S. Kathuria, S. Gaetani, D. Fegley, F. Valino, A. Duranti, A. Tontini, M. Mor, G. Tarzia, G. La Rana, A. Calignano, A. Giustino, M. Tattoli, M. Palmery, V. Cuomo, D. Piomelli, *Nat. Med.* 9 (2003) 76–81.
- [8] V. Di Marzo, S.K. Goparaju, L. Wang, J. Liu, S. Bátkai, Z. Járjai, F. Fezza, G.I. Miura, R.D. Palmiter, T. Sugiura, G. Kunos, *Nature* 410 (2001) 822–825.
- [9] T. Järvinen, D.W. Pate, K. Laine, *Pharmacol. Ther.* 95 (2002) 203–220.
- [10] L. Hanus, A. Breuer, S. Tchilibon, S. Shiloah, D. Goldenberg, M. Horowitz, R.G. Pertwee, R.A. Ross, R. Mechoulam, E. Fride, *Proc. Natl. Acad. Sci. U.S.A.* 96 (1999) 14228–14233.
- [11] V. Di Marzo, T. Bisogno, L. De Petrocellis, D. Melck, P. Orlando, J.A. Wagner, G. Kunos, *Eur. J. Biochem.* 264 (1999) 258–267.
- [12] V. Di Marzo, L. De Petrocellis, N. Sepe, A. Buono, *Biochem. J.* 316 (1996) 977–984.
- [13] B.F. Cravatt, D.K. Giang, S.P. Mayfield, D.L. Boger, R.A. Lerner, N.B. Gilula, *Nature* 384 (1996) 83–87.
- [14] T.P. Dinh, D. Carpenter, F.M. Leslie, T.F. Freund, I. Katona, S.L. Sensi, S. Kathuria, D. Piomelli, *Proc. Natl. Acad. Sci. U.S.A.* 99 (2002) 10819–10824.
- [15] S.K. Goparaju, N. Ueda, K. Taniguchi, S. Yamamoto, *Biochem. Pharmacol.* 57 (1999) 417–423.
- [16] A.H. Lichtman, E.G. Hawkins, G. Griffin, B.F. Cravatt, *J. Pharmacol. Exp. Ther.* 302 (2002) 73–79.
- [17] S.M. Saario, J.R. Savinainen, J.T. Laitinen, T. Järvinen, R. Niemi, *Biochem. Pharmacol.* 67 (2004) 1381–1387.
- [18] M. Seierstad, J.G. Breitenbucher, *J. Med. Chem.* 51 (2008) 7327–7343.
- [19] A.H. Lichtman, D. Leung, C.C. Shelton, A. Saghatelian, C. Hardouin, D.L. Boger, B.F. Cravatt, *J. Pharmacol. Exp. Ther.* 311 (2004) 441–448.
- [20] L. Chang, L. Luo, J.A. Palmer, S. Sutton, S.J. Wilson, A.J. Barbier, J.G. Breitenbucher, S.R. Chaplan, M. Webb, *Br. J. Pharmacol.* 148 (2006) 102–113.
- [21] M. Scherma, J. Medalie, W. Fratta, S.K. Vadivel, A. Makriyannis, D. Piomelli, E. Mikics, J. Haller, S. Yasar, G. Tanda, S.R. Goldberg, *Neuropharmacology* 54 (2008) 129–140.
- [22] C. Hardouin, M.J. Kelso, F.A. Romero, T.J. Rayl, D. Leung, I. Hwang, B.F. Cravatt, D.L. Boger, *J. Med. Chem.* 50 (2007) 3359–3368.
- [23] M. Mor, S. Rivara, A. Lodola, P.V. Plazzi, G. Tarzia, A. Duranti, A. Tontini, G. Piersanti, S. Kathuria, D. Piomelli, *J. Med. Chem.* 47 (2004) 4998–5008.
- [24] G. Tarzia, A. Duranti, A. Tontini, G. Piersanti, M. Mor, S. Rivara, P.V. Plazzi, C. Park, S. Kathuria, D. Piomelli, *J. Med. Chem.* 46 (2003) 2352–2360.
- [25] J.P. Alexander, B.F. Cravatt, *Chem. Biol.* 12 (2005) 1179–1193.
- [26] G.G. Muccioli, N. Fazio, G.K.E. Scriba, W. Poppitz, F. Cannata, J.H. Poupaert, J. Wouters, D.M. Lambert, *J. Med. Chem.* 49 (2006) 417–425.
- [27] K. Ahn, D.S. Johnson, L.R. Fitzgerald, M. Liimatta, A. Arendse, T. Stevenson, E.T. Lund, R.A. Nugent, T.K. Nomanbhoy, J.P. Alexander, B.F. Cravatt, *Biochemistry* 46 (2007) 13019–13030.

- [28] J.M. Keith, R. Apodaca, W. Xiao, M. Seierstad, K. Pattabiraman, J. Wu, M. Webb, M.J. Karbarz, S. Brown, S. Wilson, B. Scott, C.S. Tham, L. Luo, J. Palmer, M. Wennerholm, S. Chaplan, J.G. Breitenbucher, *Bioorg. Med. Chem. Lett.* 18 (2008) 4838–4843.
- [29] X. Wang, K. Sarris, K. Kage, D. Zhang, S.P. Brown, T. Kolasa, C. Surowy, O.F. El Kouhen, S.W. Muchmore, J.D. Brioni, A.O. Stewart, *J. Med. Chem.* 52 (2009) 170–180.
- [30] A. Minkkilä, S.M. Saario, H. Käsänen, J. Leppänen, A. Poso, T. Nevalainen, *J. Med. Chem.* 51 (2008) 7057–7060.
- [31] W. Lang, C. Qin, S. Lin, A.D. Khanolkar, A. Goutopoulos, P. Fan, K. Abouzid, Z. Meng, D. Biegel, A. Makriyannis, *J. Med. Chem.* 42 (1999) 896–902.
- [32] M.J. Myllymäki, S.M. Saario, A.O. Kataja, J.A. Castillo-Melendez, T. Nevalainen, R.O. Juvonen, T. Järvinen, A.M.P. Koskinen, *J. Med. Chem.* 50 (2007) 4236–4242.
- [33] (a) H.A. McManus, P.J. Guiry, *Chem. Rev.* 104 (2004) 4151–4202;
(b) M.J. Oila, J.E. Tois, A.M.P. Koskinen, *Tetrahedron* 61 (2005) 10748–10756.
- [34] M.J. Myllymäki, A.M.P. Koskinen, *Tetrahedron Lett.* 48 (2007) 2295–2298.
- [35] J.H. Chesterfield, J.F.H. McOmie, M.S. Tute, *J. Chem. Soc.* (1960) 4590–4596.
- [36] B. Singh, G.Y. Leshner, *Heterocycles* 31 (1990) 2163–2172.
- [37] H. Vorbrüggen, K. Krolkiewicz, *Tetrahedron* 49 (1993) 9353–9372.
- [38] I. Mohammadpour-Baltork, A.R. Khosropour, S.F. Hojati, *Synlett* (2005) 2747–2750.
- [39] (a) H. Witte, W. Seeliger, *Liebigs Ann. Chem.* (1974) 996–1009;
(b) C. Bolm, K. Weickhardt, M. Zehnder, T. Ranzz, *Chem. Ber.* 124 (1991) 1173–1180.
- [40] (a) T. Yaegashi, S. Nunomura, T. Okutome, T. Nakayama, M. Kurumi, *Chem. Pharm. Bull.* 32 (1984) 4466–4477;
(b) P.J. Reider, R.S. Eichen Conn, P. Davis, V.J. Grenda, A.J. Zambito, E.J.J. Grabowski, *J. Org. Chem.* 52 (1987) 3326–3334;
(c) Y. Huang, D.R. Dalton, P.J. Carrol, *J. Org. Chem.* 62 (1997) 372–376.
- [41] M. Mileni, D.S. Johnson, Z. Wang, D.S. Everdeen, M. Liimatta, B. Pabst, K. Bhattacharya, R.A. Nugent, S. Kamtekar, B.F. Cravatt, K. Ahn, R.C. Stevens, *Proc. Natl. Acad. Sci. U.S.A.* 105 (2008) 12820–12824.
- [42] M.H. Bracey, M.A. Hanson, K.R. Masuda, R.C. Stevens, B.F. Cravatt, *Science* 298 (2002) 1793–1796.
- [43] (a) G. Jones, P. Willett, R.C. Glen, A.R. Leach, R. Taylor, *J. Mol. Biol.* 267 (1997) 727–748;
(b) M.J. Hartshorn, M.L. Verdonk, G. Chessari, S.C. Brewerton, W.T. Mooij, P.N. Mortenson, C.W. Murray, *J. Med. Chem.* 50 (2007) 726–741.
- [44] A. Lodola, M. Mor, S. Rivara, C. Christov, G. Tarzia, D. Piomelli, A.J. Mulholland, *Chem. Commun. (Camb)* 13 (2008) 214–216.
- [45] M. Mor, A. Lodola, S. Rivara, F. Vacondio, A. Duranti, A. Tontini, S. Sanchini, G. Piersanti, J.R. Clapper, A.R. King, G. Tarzia, D. Piomelli, *J. Med. Chem.* 51 (2008) 3487–3498.
- [46] GRID, v. 22a, Molecular Discovery Ltd., Pinner, Middlesex.
- [47] M. Hendlich, *Acta Crystallogr. D. Biol. Crystallogr.* 54 (1998) 1178–1182.
- [48] J. Badger, I. Minor, M.A. Oliveira, T.J. Smith, M.G. Rossmann, *Proteins* 6 (1989) 1–19.
- [49] J.S. Murray, S. Ranganathan, P. Politzer, *J. Org. Chem.* 56 (1991) 3734–3737.
- [50] P.W. Kenny, *J. Chem. Soc., Perkin Trans. 2* (1994) 199–202.
- [51] D. Zhang, A. Saraf, T. Kolasa, P. Bhatia, G.Z. Zheng, M. Patel, G.S. Lannoye, P. Richardson, A. Stewart, J.C. Rogers, J.D. Brioni, C.S. Surowy, *Neuropharmacology* 52 (2007) 1095–1105.
- [52] V.V. Somayajulu, N.V. Subba Rao, *Proc. Indian Acad. Sci. Sect. A* 59 (1964) 396–402.
- [53] S.M. Johnson, S. Connelly, I.A. Wilson, J.W. Kelly, *J. Med. Chem.* 51 (2008) 260–270.
- [54] T.-Y. Shen, R.L. Clark, A.A. Pessolano, B.E. Witzel, T.J. Lanza, US 4038396, 1977, CAN 90:137799.
- [55] T.J. Kress, *J. Org. Chem.* 50 (1985) 3073–3076.
- [56] F. Dennin, D. Blondeau, H. Sliwa, *J. Heterocycl. Chem.* 27 (1990) 1963–1967.
- [57] J.F. McOmie, A.B. Turner, *J. Chem. Soc.* (1963) 5590–5593.
- [58] J. Luston, J. Kronek, F. Bohme, *J. Polym. Sci. Part A: Polym. Chem.* 44 (2005) 343–355.
- [59] M. Bradford, *Anal. Biochem.* 72 (1976) 248–254.
- [60] A. Lorenzen, M. Fuss, H. Vogt, U. Schwabe, *Mol. Pharmacol.* 44 (1993) 115–123.
- [61] K.M. Kurkinen, J. Koistinaho, J.T. Laitinen, *Brain Res.* 769 (1997) 21–28.
- [62] J.R. Savinainen, T. Järvinen, K. Laine, J.T. Laitinen, *Br. J. Pharmacol.* 134 (2001) 664–672.
- [63] S.M. Saario, A. Poso, R.O. Juvonen, T. Järvinen, O.M.H. Salo-Ahen, *J. Med. Chem.* 49 (2006) 4650–4656.
- [64] S.M. Saario, O.M. Salo, T. Nevalainen, A. Poso, J.T. Laitinen, T. Järvinen, R. Niemi, *Chem. Biol.* 12 (2005) 649–656.
- [65] S.C. Lovell, J.M. Word, J.S. Richardson, D.C. Richardson, *Proteins* 40 (2000) 389–408.
- [66] J.M. Wang, P. Cieplak, P.A. Kollman, *J. Comput. Chem.* 21 (2000) 1049–1074.
- [67] Sybyl v. 8.1; Tripos Associates, Inc.: St. Louis, MO.
- [68] (a) <http://molprobiy.biochem.duke.edu/> (retrieved 01.03.09);
(b) S.C. Lovell, I.W. Davis, W.B. Arendall, P.I. de Bakker, J.M. Word, M.G. Prisant, J.S. Richardson, D.C. Richardson, *Proteins* 50 (2003) 437–450.
- [69] M.K. McKinney, B.F. Cravatt, *J. Biol. Chem.* 278 (2003) 37393–37399.
- [70] T.A. Halgren, *J. Comput. Chem.* 17 (1996) 490–519.
- [71] M.J. Frisch, G.W. Trucks, H.B. Schlegel, G.E. Scuseria, M.A. Robb, J.R. Cheeseman, J.A. Montgomery, T. Vreven, K.N. Kudin, J.C. Burant, J.M. Millam, S.S. Iyengar, J. Tomasi, V. Barone, B. Mennucci, M. Cossi, G. Scalmani, N. Rega, G.A. Petersson, H. Nakatsuji, M. Hada, M. Ehara, K. Toyota, R. Fukuda, J. Hasegawa, M. Ishida, T. Nakajima, Y. Honda, O. Kitao, H. Nakai, M. Klene, X. Li, J.E. Knox, H.P. Hratchian, J.B. Cross, V. Bakken, C. Adamo, J. Jaramillo, R. Gomperts, R.E. Stratmann, O. Yazyev, A.J. Austin, R. Cammi, C. Pomelli, J.W. Ochterski, P.Y. Ayala, K. Morokuma, G.A. Voth, P. Salvador, J.J. Dannenberg, V.G. Zakrzewski, S. Dapprich, A.D. Daniels, M.C. Strain, O. Farkas, D.K. Malick, A.D. Rabuck, K. Raghavachari, J.B. Foresman, J.V. Ortiz, Q. Cui, A.G. Baboul, S. Clifford, J. Cioslowski, B.B. Stefanov, G. Liu, A. Liashenko, P. Piskorz, I. Komaromi, R.L. Martin, D.J. Fox, T. Keith, M.A. Al-Laham, C.Y. Peng, A. Nanayakkara, M. Challacombe, P.M.W. Gill, B. Johnson, W. Chen, M.W. Wong, C. Gonzalez, J.A. Pople, *Gaussian 03, Revision B.04*, Gaussian, Inc., Wallingford, CT, 2004.
- [72] W. Humphrey, A. Dalke, K. Schulten, *J. Mol. Graphics* 14 (1996) 33–38 pp. 27–28.